


# Divergent locomotor evolution in “giant” kangaroos: Evidence from foot bone bending resistances and microanatomy

Amber Y. Wagstaffe<sup>1,2</sup>  | Adrian M. O'Driscoll<sup>1,3</sup> | Callum J. Kunz<sup>1</sup> | Emily J. Rayfield<sup>1</sup> | Christine M. Janis<sup>1,4</sup>

<sup>1</sup>Department of Earth Sciences, University of Bristol, Bristol, UK

<sup>2</sup>Energy and Environment Institute, University of Hull, Hull, UK

<sup>3</sup>Center for Anatomical and Human Studies, Hull York Medical School, University of York, York, UK

<sup>4</sup>Department of Ecology and Evolutionary Biology, Brown University, Providence, Rhode Island, USA

## Correspondence

Amber Y. Wagstaffe, Energy and Environment Institute, University of Hull, Hull, HU6 7RX, UK.

Email: a.wagstaffe-2020@hull.ac.uk

## Funding information

Bushnell Foundation; University of Bristol MSc Program in Palaeobiology

## Abstract

The extinct sthenurine (giant, short-faced) kangaroos have been proposed to have a different type of locomotor behavior to extant (macropodine) kangaroos, based both on physical limitations (the size of many exceeds the proposed limit for hopping) and anatomical features (features of the hind limb anatomy suggestive of weight-bearing on one leg at a time). Here, we use micro computerised tomography (micro-CT) scans of the pedal bones of six kangaroos, three sthenurine, and three macropodine, ranging from ~50 to 150 kg, to investigate possible differences in bone resistances to bending and cortical bone distribution that might relate to differences in locomotion. Using second moment of area analysis, we show differences in resistance to bending between the two subfamilies. Distribution of cortical bone shows that sthenurines had less resistant calcaneal tubers, implying a different foot posture during locomotion, and the long foot bones were more resistant to the medial bending stresses. These differences were the most pronounced between Pleistocene monodactyl sthenurines (*Sthenurus stirlingi* and *Procoptodon browneorum*) and the two species of *Macropus* (the extant *M. giganteus* and the extinct *M. cf. M. titan*) and support the hypothesis that these derived sthenurines employed bipedal striding. The Miocene sthenurine *Hadronomas* retains some more macropodine-like features of bone resistance to bending, perhaps reflecting its retention of the fifth pedal digit. The Pleistocene macropodine *Protemnodon* has a number of unique features, possibly indicative of a type of locomotion unlike the other kangaroos.

## KEYWORDS

bone resistance to bending, locomotion, Macropodinae, pedal anatomy, Sthenurinae

## 1 | INTRODUCTION

Macropodoidea (Diprotodontia: Marsupialia) is a diverse superfamily of kangaroos and related forms found in Australia and New Guinea (Burk et al., 1998; see Figure 1). There is no fossil record of macropodoids until the late Oligocene, but molecular data indicate

divergence from possum-like animals (phalangeroids) in the Eocene (Burk & Springer, 2000; Mitchell et al., 2014; Llamas et al., 2015). The fossil record shows diversification of basal macropodoids in the early to middle Miocene, and both fossil and molecular data pick up the diversification of the extant lineages in the Plio-Pleistocene (Couzens & Prideaux, 2018; Mitchell et al., 2014).

This is an open access article under the terms of the Creative Commons Attribution-NonCommercial License, which permits use, distribution and reproduction in any medium, provided the original work is properly cited and is not used for commercial purposes.

© 2022 The Authors. *Journal of Morphology* published by Wiley Periodicals LLC.

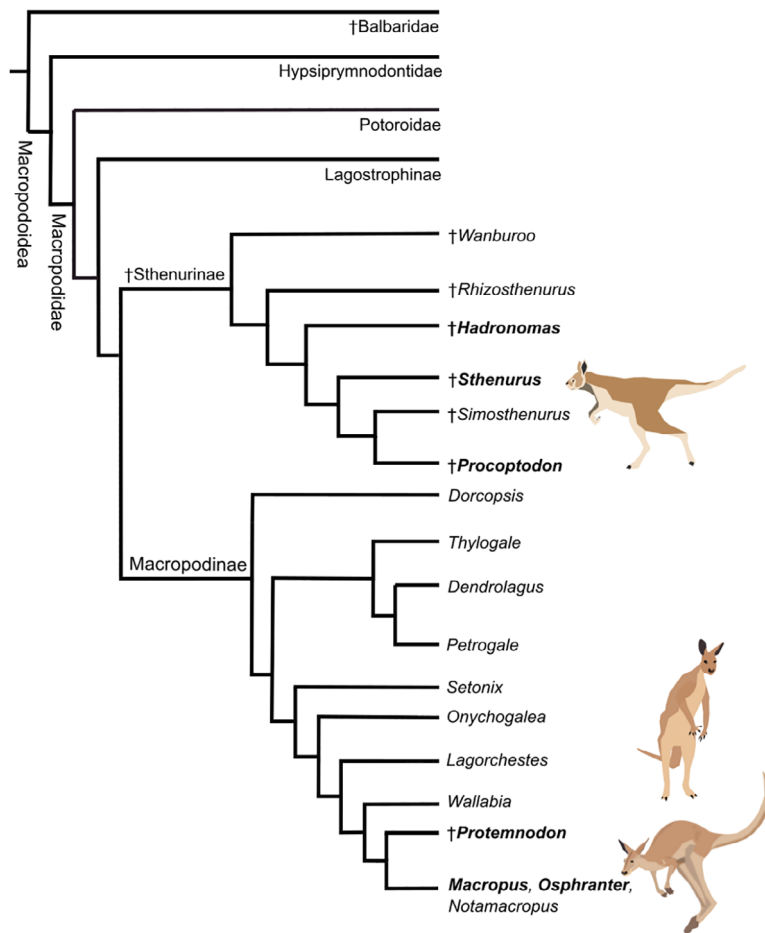


**FIGURE 1** Simplified phylogeny of the Macropodiformes (modified from Llamas et al., 2015). A dagger (†) indicates an extinct taxon. Taxa included in this study are in boldface. Drawings by Billie Jones, credits for the drawings as follows: *S. stirlingi* modified from Brian regal in Janis et al. (2014), with permission; *Protemnodon anak* modified from a photograph taken by CMJ of the mounted skeleton at the South Australian Museum; *Osphranter Rufus* created from composite images in the public domain

Macropodoidea is composed of around 60 extant and over 60 fossil taxa (Jackson & Vernes, 2010; Prideaux & Warburton, 2010a). Macropodoidae comprises the crown group of the three extant families (see Prideaux & Warburton, 2010a; Llamas et al., 2015); a further extinct family, Balbaridae, may lie outside of this grouping (with the total group then being Macropodiformes), or Balbaridae may be the sister taxon to the Hypsiprymnodontidae (Den Boer & Kear, 2018; Kear & Cooke, 2001). The Hypsiprymnodontidae (today containing only the musky rat-kangaroo, *Hypsiprymnodon moschatus*), the Potoroidae (rat-kangaroos, three extant genera, and eight extant species), and Macropodidae (kangaroos and wallabies, 11 extant genera, and 63 extant species) are crownward sister taxa (see Figure 1).

Within the Macropodidae there are three subfamilies: the basal Lagostrophinae (today containing only the banded hare-wallaby *Lagostrophus fasciatus*: Prideaux & Warburton, 2010a; Llamas et al. 2015), the Macropodinae (all other extant macropodids), and the extinct Sthenurinae (3–5 genera and ~25 species, see Prideaux, 2004, the larger Plio-Pleistocene forms are often referred to as “giant, short-faced kangaroos”); note that some authors claim that *Lagostrophus* is in fact a basal sthenurine (Cascini et al., 2019; Westerman et al., 2002).

The sthenurines are the focus of this study. Previous research (Janis et al., 2014) proposed, on the basis of comparisons of gross macropodid osteological anatomy, that sthenurines employed a

bipedal striding mode of locomotion, certainly as an alternative to slow quadrupedal (or pentapedal) locomotion, and likely also as an alternative to hopping in larger species. This study investigates details of bone microanatomy, including both calculation of resistances to foot bone bending (second moment of area analyses) and relative distribution of cortical bone within the bones. We aim to determine whether similar signatures of locomotor differences between macropodines and sthenurines occur at this level of investigation.

## 1.1 | Comparisons of macropodid anatomies and body sizes

Sthenurines differ from macropodines in numerous features of their craniodental and postcranial anatomy (see Wells & Tedford, 1995). Craniodentally, sthenurines have a dentition specialized for browsing and the Plio-Pleistocene forms have shorter faces than macropodines (Mitchell & Wroe, 2019). In the postcranial skeleton, the Plio-Pleistocene taxa (principally *Procoptodon*, *Sthenurus*, and *Simosthenurus*) reduce the fifth pedal digit to a proximal metapodial remnant, rendering them monodactyl. Other postcranial differences (in relation to the pedal bones considered in this paper) include: a calcaneum with a shorter and broader tuber in sthenurines, especially at the tip, the tuber directed slightly anteriorly rather than slightly posteriorly as in macropodines,

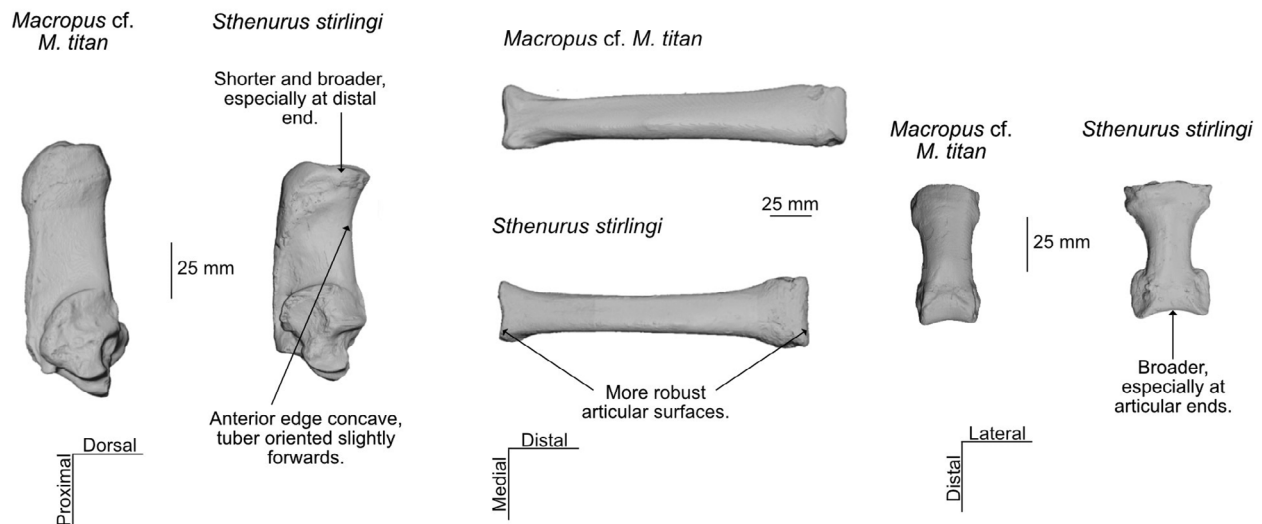


**FIGURE 2** Comparison of pedal bone morphologies of macropodines (*Macropus* cf. *M. titan*) and sthenurines (*S. stirlingi*); images produced from volume-rendered CT scans. From left to right: Calcanea in lateral view; fourth metatarsals in cranial view; proximal fourth pedal phalanges in cranial view. Images of *M. cf. M. titan* reversed so that all bones appear to be left side ones

and with a concave anterior profile; a more robust fourth metatarsal in sthenurines, with a broader articular surfaces (at least in the monodactyl taxa); and phalanges with a characteristic “I-beam” shape in sthenurines, with laterally expanded epiphyses (see Janis et al., 2014; Murray, 1995; Wells & Tedford, 1995) (see Figure 2). The proximal phalanx in extant large species of *Macropus* and *Osphranter* is also elongated relative to the sthenurine condition, but this is not the case in all macropodines and this bone is not as greatly elongated in *Macropus* cf. *M. titan* as in extant large kangaroos (see Figure 2; Jones, 2020).

While sthenurines are often termed “giant” kangaroos (i.e., larger than macropodines, which range in body mass from 1.5–90 kg) this is not true of the entire family. The most basal sthenurines are the middle Miocene *Wanburoo hilarus* (~8 kg; Butler et al., 2021) and early late Miocene *Rhizosthenurus flanneryi* (~26 kg; this paper), but both were large members of the macropodoid community of the time (Butler et al., 2017). Later sthenurines continued this trend of being large macropodids: the late Miocene (~8 Ma) *Hadronomas* was ~73 kg (this paper), while the Plio-Pleistocene taxa ranged from ~50 kg in *Procoptodon gilli* to ~230 kg in *Procoptodon goliath* (Helgen et al., 2006).

*P. goliath* is the standard sthenurine “poster child,” popularly cited as being over three meters in height. But *P. goliath* was exceptionally large for a sthenurine: the “average” sthenurine would have been something more like *Simosthenurus occidentalis*, at a body mass of ~120 kg (Helgen et al., 2006; estimated here at ~113 kg). Nevertheless, this is considerably larger than the largest kangaroos today: while a male red kangaroo, *Osphranter rufus*, can weigh as much as 90 kg, the average mass of adult males of the large species of the *Macropus* complex species (*Macropus*, *Osphranter*, and *Notamacropus*) is around 40 kg (Helgen et al., 2006); that is, a little smaller than the smallest Plio-Pleistocene sthenurine.

However, a few very large macropodines existed in the Pleistocene: *Macropus titan* had an estimated body mass of 150 kg (Helgen et al., 2006), *Macropus ferragus* was a similarly-sized large species, and recently fragmentary material has provided a body mass estimate of ~274 kg for a new giant Pleistocene macropodine (an unnamed species of *Macropus*), larger than the largest known sthenurine (Hocknull et al., 2020). In addition to Pleistocene species of *Macropus*, the related extinct genus *Protemnodon* also attained sizes much larger than extant macropodines, with the larger Pleistocene species ranging from ~110 to ~166 kg (Helgen et al., 2006).

Estimation of body masses of extinct taxa is problematic, especially if these taxa range outside of the size of the extant taxa that can form a reference group (e.g., Campione & Evans, 2012). We shall later present our own estimations of the body masses of some of the extinct kangaroo taxa.

## 1.2 | Kangaroo locomotion and the problems of large body size

Extant macropods are renowned for their mode of rapid locomotion—bipedal hopping (also known as saltation or ricochet locomotion). This is reflected in their distinctive, enlarged hind limbs, and their highly specialized feet (Jackson & Vernes, 2010). The tibia of macropodoids is unusually long (tree-kangaroos are an exception), and its length scales with strong positive allometry, while the length of the femur and fourth metatarsal scale more or less with isometry (Doubé et al., 2018; McGowan, Skinner, & Biewener, 2008).

Kangaroo feet are dominated by the fourth digit, which is the main weight-bearing element, although the fifth digit is also weight-bearing to some extent. The fifth metatarsal is usually considerably

less robust than the fourth one (but is relatively robust in tree-kangaroos; Warbuton et al., 2012), and is slightly shorter; the phalanges of the fifth pedal digit are similar in form to those of the fourth, but smaller in size. The fifth digit is reduced to a metatarsal splint in the Plio-Pleistocene sthenurines. The first digit has been lost in all extant taxa crownward of the Hypsiprymnodontidae, and in all macropodoids the second and third digits have been reduced to splint-like syndactylous elements (as in other members of the Diprotodontia). The metatarsals are relatively long, as in cursorial mammals in general (again, tree-kangaroos are an exception), and the posture of the hind foot during locomotion is digitigrade, although kangaroos can stand with a plantigrade foot posture.

All extant species of macropodoids can hop, except for the musky rat-kangaroo, although some smaller species favor quadrupedal bounding as a rapid gait (Windsor & Dagg, 1971). At slower speeds, a gait where the forelimbs bear weight is employed in all extant forms, with larger species among the clade including *Wallabia*, *Onychogalea*, and the *Macropus* complex (see Figure 1), adopting a specialized pentapedal walk (where the tail is used as a fifth limb) (Dawson et al., 2015). Quadrupedal or pentapedal gaits are employed at slow speeds due to the biomechanical difficulties and high energetic costs associated with hopping slowly (Dawson, 1983; O'Connor et al., 2014); but such gaits are energetically expensive, and increasing speed is achieved by increases in stride frequency rather than increases in stride length (Dawson & Taylor, 1973). Conversely, at higher speeds, hopping is remarkably energy efficient, particularly in large species of *Macropus* and *Osphranter*, where the energetic cost of transport in large kangaroos are less than a third than those of a quadruped of similar size (Baudinette et al., 1992). In large macropodoids energetic costs of locomotion are uncoupled from speed, and speed increases via increasing stride length (Dawson & Taylor, 1973). This decoupling of energetic costs and speeds also appears to hold for smaller macropodoids (~5 kg) such as the tamar wallaby (*Notamacropus eugenii*) and the red-bellied pademelon (*Thylogale billardieri*), but not for the potoroids (1–3 kg; see Table S4.3) (Bennett, 2000). The energetic benefits of bipedal hopping may only be available to animals over ~4 kg (Baudinette, 1994).

Larger macropods achieve high levels of energy efficiency during hopping through the recovery of elastic energy in the hind limb extensor tendons of the gastrocnemius, plantaris (=flexor digitorum superficialis), and flexor digitorum profundus muscles (Baudinette et al., 1992; Biewener & Baudinette, 1995; Pollock & Shadwick, 1994; Snelling et al., 2017). Energy savings differ depending on size and speed but are most effective in large species of *Macropus* and *Osphranter*, where 50% or greater amounts of energy may be recovered (Cavagna et al., 1977). To maximize energy savings tendons must be long and/or slender, and capable of extension, but they must also withstand mechanical stresses to avoid rupture (Biewener, 2008).

As the cross-sectional area of the hind limb extensor tendons scales with negative allometry in kangaroos (while hind limb extensor muscle mass and muscle physiological cross-sectional area scale with positive allometry), larger kangaroos have relatively thinner tendons (McGowan, Skinner, & Biewener, 2008). This allows for a greater

amount of elastic energy storage but at the expense of tendon safety factors (i.e., the strength of tendon relative to the experienced load), and large red kangaroos may experience tendon safety factors as low as 1.1 during hopping (where failure would occur if the safety factor was less than one) (McGowan, Skinner, & Biewener, 2008). Consequently, there is a hypothesized optimum size range of 50–60 kg for hopping kangaroos (Bennett & Taylor, 1995), and an estimated upper body size limit of 140–160 kg (McGowan, Skinner, & Biewener, 2008; Snelling et al., 2017). This impacts on our understanding of the possible locomotor behavior of the largest sthenurines. McGowan, Skinner, and Biewener (2008) predicted that *P. goliath*, at an estimated body mass of 250 kg (Helgen et al., 2006), would have a tendon safety factor of ~0.89 during hopping; this would clearly not be a viable locomotor situation.

Note that it is possible for kangaroos to evolve relatively thicker tendons that have a higher safety factor, as seen in the yellow-footed rock wallaby (*Petrogale xanthopus*); this morphology allows the animal to withstand the high forces generated by the acceleration and jumping, greater than those encountered during steady-speed hopping. But rock wallabies have a reduced capacity for elastic energy storage during hopping—the similarly-sized tamar wallaby (*N. eugenii*) stores up to 73% more elastic strain energy (McGowan, Baudinette, & Biewener, 2008b). Thus, thicker tendons would not solve the locomotor problems of large hopping kangaroos; they might allow for some limited hopping, but not the sort of rapid hopping seen in extant large kangaroos.

Increasing body size poses problems for locomotion in all animals. The laws of physics would predict that bone and muscle cross-sectional area scale with positive allometry, but this would render larger animals proportionally heavier. Instead, these features actually scale with near isometry (slight positive allometry) up to a body mass of around 300 kg (Biewener, 2005; Dick & Clemente, 2017). Mammals up to this size limit cope with increasing body size by adjusting their posture, assuming an increasingly erect posture with less flexed limbs at larger sizes (Biewener, 2005). This increases the mechanical advantage (EMA) of the limbs, mitigating the effect of increasing ground reaction forces at larger body size by decreasing the forces experienced at the joints; however, this postural change may come at the expense of decreased agility (Biewener, 2005; Dick & Clemente, 2017). Beyond a body mass of 300 kg the maximum postural change has been achieved, and at larger sizes than this, strong positive allometry of bone and muscle cross-sectional area in mammals is now followed (Biewener, 2005).

The issue of postural change is where hopping locomotion at larger body sizes poses a particular problem: while quadrupedal mammals attain more erect postures, hopping mammals must maintain a more crouched one. In addition, the ground reaction forces experienced by bipedal hoppers are larger than those of quadrupedal animals of a comparable size, as bipedal hoppers must generate higher propulsive forces per limb (Blickhan & Full, 1993). Large extant macropods remain crouched during locomotion regardless of body size, due to the requirement of a flexed-leg posture for hopping, and so are unable to alter the limb EMA across body size (Bennett & Taylor, 1995; McGowan, Skinner, & Biewener, 2008). This is why there are body size limits on hopping locomotion.

During the Plio-Pleistocene, numerous species of kangaroo were above the optimum body size range for hopping (i.e., ~50 kg, Bennett & Taylor, 1995), and some were even above the proposed body size limit (i.e., ~150 kg, McGowan, Skinner, & Biewener, 2008; Snelling et al., 2017), rendering hopping limited or impossible: this included many species within the Sthenurinae, as well as species of *Macropus* and *Protemnodon* within the Macropodinae. Based on aspects of their hind limb anatomy, as well as consideration of these body mass issues, Janis et al. (2014) proposed that sthenurines employed bipedal striding as a locomotor gait. This gait would have occurred at least in addition to hopping (especially in the smaller species), if not entirely replacing hopping locomotion. In particular, striding was most likely employed as a slow gait rather than quadrupedal or pentapedal locomotion, and sthenurines appear to have had limited capacity for

weight-bearing on their forelimbs (Janis et al., 2020; Jones, 2020). A recent discovery of a Pliocene trackway has confirmed the proposal that sthenurines could locomote via bipedal striding (Camens & Worthy, 2019), although of course trackway data cannot refute the use of hopping in addition to striding.

Here, we employ data from bone microanatomy and biomechanical analysis from micro computerised tomography (micro-CT) scans of kangaroo pedal bones to further investigate the locomotor abilities of sthenurines in comparison with macropodines, and to address the hypothesis of bipedal striding in sthenurines. We calculated bending stresses and torsion along the lengths of the bones by means of second moment of area analysis; we did not consider the issues raised by Bertram and Biewener (1988) relating to bone curvature, as all of the long bones examined here exhibit little curvature, and the main

**TABLE 1** Specimens used in analyses

Subfamily	Taxon	Element	Specimen #	Estimated body mass
Macropodinae	<i>Macropus</i> cf. <i>M. †titan</i>	R calcaneum	NHMUK-PV M10702a	176 kg
		L fourth metatarsal	NHMUK-PV M5000	
		R prox. phalanx	NHMUK-PV M3456a	
		R inter. phalanx	NHMUK-PV M3456b	
Macropodinae	<i>Macropus giganteus</i>	L calcaneum	AMNH 2390	54 kg
		L fourth metatarsal	AMNH 2390	
		L prox. phalanx	AMNH 2390	
		L inter. phalanx	AMNH 2390	
Macropodinae	† <i>Protemnodon brehus</i>	L calcaneum	AMNH 145501	97 kg
		L fourth metatarsal	AMNH 145501	
		L prox. phalanx	AMNH 145501	
		L inter. phalanx	AMNH 145501	
Macropodinae	<i>Osphranter rufus</i>	L fourth metatarsal	UMZC A112.31/3	36 kg
		L fifth metatarsal	UMZC A112.31/3	
†Sthenurinae	† <i>Sthenurus stirlingi</i>	L calcaneum	AMNH 117494	164 kg
		L fourth metatarsal	AMNH 117494	
		L prox. phalanx	AMNH 117494	
		L inter. phalanx	AMNH 117494	
†Sthenurinae	† <i>Procoptodon browneorum</i>	L calcaneum	WAM 65.4.78	52 kg
		L fourth metatarsal	WAM 62.3.637	
		R prox. phalanx	WAM 68.4.643	
		L inter. phalanx	WAM 63.3.642	
†Sthenurinae	† <i>Hadronomas puckeridgei</i>	L calcaneum	NTM P9336	73 kg
		R calcaneum	NTM P10115	
		R fourth metatarsal	NTM P9214	
		L fifth metatarsal	NTM P8714-22	
		L prox. phalanx	NTM P9051	
		R inter. phalanx	NTM P6315	

*Note:* Body mass estimates are mean ones, from the combined estimates from several pedal bones (see Data S1 for more detail): an alternative mass estimate for *S. stirlingi* is 176 kg (see Data S1). †, extinct taxon; inter, intermediate; L, left; prox., proximal; R, right.

Abbreviations: AMNH, American Museum of Natural History, New York, NY, USA; NHMUK-PV, Natural History Museum (Paleontology, Vertebrates), London, UK; NTM, Museum and Art Galleries of the Northern Territory, Alice Springs, WA, Australia; UMCZ, University Museum of Comparative Zoology, Cambridge, UK; WM, Western Australian Museum, Perth, WA, Australia.

portion of the calcaneum (the talus) is not a weight-bearing element. We also examined the amount and distribution of cortical bone thickness in certain pedal bones; the calcaneum, the fourth metatarsal, and the fourth proximal phalanx.

The geometry of cortical bone plays an important role in the bone's resistance to bending and torsion; species that have bones with thicker cortices experience less stress. Robusticity of bones and the thickness of cortices have been associated with primates using different types of gaits (Jashashvili et al., 2015; Kimura, 2003; Marchi, 2005). We would thus expect to see differences in the amount and distribution of cortical bone within the hind limb bones of kangaroos employing different types of gaits. In particular, we might expect to see greater resistance to stress on the medial side of the foot bones in animals that were bearing weight on leg at a time, as seen in the medial shifting of weight-bearing in humans (Aiello & Dean, 1990; Harcourt-Smith & Aiello, 2004).

Issues relating to allometry and absolute size differences in the comparison of different individuals are averted to a large extent by making matched-mass pairwise comparisons of species in the two subfamilies (our estimation of body masses is described in a later section), although we did perform size-adjustments on the data. Table 1 shows the taxa studied and their estimated body masses (and see later discussion about the estimation of body masses). Note that *Protemnodon* has been proposed to be primarily quadrupedal rather than a hopper (Den Boer, 2018; Jones, 2020); while the Plio-Pleistocene sthenurines have been proposed to engage in bipedal striding (Janis et al., 2014) the locomotion of *Hadronomas* has not been investigated.

## 2 | MATERIALS AND METHODS

### 2.1 | Materials

We studied the pedal bones, that is, calcaneum, fourth metatarsal, fourth proximal phalanx, and fourth intermediate phalanx, of three macropodines (one extant and two extinct) and three sthenurines. We also studied the fifth metatarsal of the sthenurine *Hadronomas puckeridgei* and the extant macropodine *O. rufus* (the red kangaroo).

The sthenurine *Sthenurus stirlingi* (likely a male, according to Wells & Tedford, 1995), and the macropodines *Macropus giganteus* (the eastern gray kangaroo) and *Protemnodon brehus*, all represent articulated left feet from single specimens. *S. stirlingi* and *P. brehus* are both from Lake Callabonna (Millyera Formation, medial Pleistocene of South Australia). (Note that the AMNH specimen is formally only identified as *Protemnodon* sp., but *P. brehus* is the sole *Protemnodon* species recorded from that locality [G. Prideaux, personal communication to CMJ].) The sthenurines *H. puckeridgei* and *Procoptodon browneorum*, and the macropodine *Macropus* cf. *M. titan*, are composite specimens, but the elements are of comparable size. The specimens of *H. puckeridgei* and *P. browneorum* each come from a single locality, respectively Alcoota (late Miocene of the Northern Territory) and Mammoth Cave (late Pleistocene of West Australia).

The provenance of *M. cf. M. titan* is more difficult to determine, due to these elements being collected in the late 19th century.

(Although these particular bones are identified only as “*Macropus*,” other large macropodid bones in the NMHUK-PV collections from similar times and areas have been named as *M. titan*, and so we have designated these bones as *M. cf. M. titan*. Note that the precise taxonomic identity of these bones is not important—they clearly belong to a giant macropodine kangaroo.) The bones all appear to be from the same, or similar, depositional environments. The two phalanges were collected in Queensland in 1886, and the metatarsal in Queensland in 1884. No information is available for the calcaneum. As each pedal bone is compared separately across the taxa, and in no case is the entire foot considered as a unit, it does not matter if the elements do not belong to a single individual.

### 2.2 | Digital reconstruction

Specimens were micro-CT scanned. *M. giganteus* and *S. stirlingi* were scanned at the American Museum of Natural History, New York, USA, and the other taxa were scanned at the University of Bristol, Bristol, UK. Digital segmentation and repair were performed in Avizo 8 as necessary. Reconstructed bones were saved as .TIFF files.

### 2.3 | Second moment of area

Second moment of area is a measure of the geometry of the cross-section of a beam (such as bone) that provides quantitative data on the resistance of the beam to bending. It is calculated in such a way that the distance that material (e.g., cortical bone) is placed from the neutral axis of bending has a significant impact on the values of resistance. The sum of resistance to bending in the two main axes of the beam can additionally be used to calculate the polar moment of inertia, which is a measure of the beam's resistance to torsion.

Using BoneJ (see Doube et al., 2010) data prepared for cortical bone thickness analysis were then reversed if necessary (using the “reverse tool”), to ensure all stacks were orientated proximally-distally. The axes of these data were corrected to “cranio-caudal” (=“dorso-plantar”) and “medio-lateral” and aligned with the bone. The image stacks were scaled with the relevant voxel size as the known distance using the “Set Scale ...” tool from the “Analyze” menu. The scale was set for voxel sizes using the “Set Scale” tool or “Properties” function (the voxel sizes are given in Table S1). Second moment of area about the cranio-caudal and medio-lateral axes was measured using the “Slice Geometry” function (the scan parameters for each taxon and each bone are provided in Table S2).

As there is often confusion regarding the nomenclature used when discussing second moment of area, a note is provided here for the sake of clarity. The labels,  $I_{CC}$  and  $I_{ML}$ , refer to the axes about which the bending rigidity is calculated, not the direction of applied bending, which acts perpendicularly to the axis of bending rigidity. In this way,  $I_{CC}$  refers to the second moment of area about the cranio-caudal axis, and therefore resistance to a bending stress applied in the medio-lateral direction (i.e., perpendicular to the cranio-caudal axis).

Similarly,  $I_{ML}$  refers to resistance to stress applied in the cranio-caudal direction.

Data were then exported to Microsoft Excel and used to calculate the polar moment of inertia for each of the bones. Additional columns were created in Microsoft Excel for percentage bone length (0% is proximal, and 100% is distal), to account for the differences in the slice number between the scans (see Table S2). The data were size-corrected by taking the fourth root, as second moment of area has units of  $\text{mm}^4$ : in so doing we followed the methodology of McHorse et al. (2017), rather than that of Doube et al. (2018), and did not further divide by bone length (the lengths of the calcaneal heel and the first phalanges are notably longer in extant large macropodines than in sthenurines and we did not want to overcompensate for this difference). We also did not attempt to correct for phylogeny, due to both the small sample size and the fact that we are comparing pairs of taxa of different lineages but of similar sizes (see above).

Using Microsoft Excel, for each of the four bones, mean second moment of area values were calculated for total bone length (0%–100% bone length), a proximal section (0%–25%), a midshaft section (25%–75%), and a distal section (75%–100%). These categories were selected with regard to quantitatively comparing the second moment of area values proximal, distal, and midshaft regions for each of the four bones. For each macropodine and sthenurine pair

(*Macropus* cf. *M. titan*, *S. stirlingi*; *M. giganteus*, *P. browneorum*; *P. brehus*, *H. puckeridgei*) a ratio of the mean values from each section was calculated for ease of comparison. Ratio values in the range [0.9–1.1] were considered approximately equal. Table 2 summarizes the overall results, and Tables S3.1–S3.4 show the actual values.

## 2.4 | Osteological cross-sections

We investigated the thickness and distribution of cortical bone by examining osteological cross-sections of the pedal bones. The points along the bone selected for examination were determined based on functional anatomical considerations. The sections of the calcanea were taken at 84% of the bone length (proximal to distal; i.e., near the top of the tuber), which is approximately the point of the junction between the epiphysis and the diaphysis. The sections of the metatarsals were taken at 23% of bone length (i.e., near the articulation with the tarsus), corresponding to the prominent cranio-medial ridge seen in *S. stirlingi*. The sections of the proximal phalanx (only *S. stirlingi* and *M. cf. M. titan* were included) were taken at 64% of the bone length, at the point where the sthenurine phalanx commences widening into its characteristic I-beam shape.

Reconstructed data were viewed in Avizo 8 in the XY axis using the label editor, and the volume-rendered bone was annotated to

**TABLE 2** Summary of mean second moment of area differences between pairs of species

	$I_{CC}$ (=ML resistance)	$I_{ML}$ (=CC resistance)	$J$ (=torsion)
Total bone length			
Calcaneum	<b>Mt</b> > Ss, Mg ≈ Pn, <b>Pb</b> > Hp	<b>Mt</b> > Ss, Mg ≈ Pn, <b>Pb</b> > Hp	<b>Mt</b> > Ss, Mg ≈ Pn, <b>Pb</b> > Hp
Fourth metatarsal	<b>Mt</b> > Ss, Mg < <b>Pn</b> , <b>Pb</b> > Hp	Mt ≈ Ss, Mg ≈ Pn, <b>Pb</b> < <b>Hp</b>	Mt = Ss, Mg = Pn, <b>Pb</b> ≈ Hp
Prox. phalanx	Mt < Ss, Mg < <b>Pn</b> , <b>Pb</b> ≈ Hp	<b>Mt</b> > Ss, Mg ≈ Pn, <b>Pb</b> = Hp	Mt ≈ Ss, Mg < <b>Pn</b> , <b>Pb</b> ≈ Hp
Inter. phalanx	Mt < Ss, Mg < <b>Pn</b> , <b>Pb</b> ≈ Hp	Mt < Ss, Mg < <b>Pn</b> , <b>Pb</b> ≈ <Hp	Mt < Ss, Mg < <b>Pn</b> , <b>Pb</b> ≈ Hp
Proximal section (0%–25% bone length)			
Calcaneum	<b>Mt</b> > Ss, <b>Mg</b> > Pn, <b>Pb</b> > Hp	<b>Mt</b> > Ss, <b>Mg</b> > Pn, <b>Pb</b> > Hp	<b>Mt</b> > Ss, <b>Mg</b> > Pn, <b>Pb</b> > Hp
Fourth metatarsal	<b>Mt</b> > Ss, Mg < <b>Pn</b> , <b>Pb</b> > Hp	Mt < Ss, <b>Mg</b> > Pn, <b>Pb</b> < <b>Hp</b>	Mt ≈ Ss, Mg ≈ Pn, <b>Pb</b> ≈ Hp
Prox. phalanx	Mt < Ss, Mg < <b>Pn</b> , <b>Pb</b> < <b>Hp</b>	<b>Mt</b> > Ss, Mg < <b>Pn</b> , <b>Pb</b> < <b>Hp</b>	Mt = Ss, Mg < <b>Pn</b> , <b>Pb</b> < <b>Hp</b>
Inter. phalanx	Mt < Ss, Mg < <b>Pn</b> , <b>Pb</b> < <b>Hp</b>	Mt < Ss, Mg < <b>Pn</b> , <b>Pb</b> < <b>Hp</b>	Mt < Ss, Mg < <b>Pn</b> , <b>Pb</b> < <b>Hp</b>
Midshaft section (25%–75% bone length)			
Calcaneum	<b>Mt</b> > Ss, Mg < <b>Pn</b> , <b>Pb</b> > Hp	<b>Mt</b> > Ss, <b>Mg</b> > Pn, <b>Pb</b> > Hp	<b>Mt</b> > Ss, Mg ≈ Pn, <b>Pb</b> > Hp
Fourth metatarsal	<b>Mt</b> > Ss, Mg ≈ Pn, <b>Pb</b> > Hp	Mt < Ss, <b>Mg</b> > Pn, <b>Pb</b> < <b>Hp</b>	Mt ≈ Ss, Mg ≈ Pn, <b>Pb</b> ≈ Hp
Prox. phalanx	Mt ≈ Ss, Mg < <b>Pn</b> , <b>Pb</b> > Hp	<b>Mt</b> > Ss, <b>Mg</b> > Pn, <b>Pb</b> > Hp	Mt ≈ Ss, Mg < <b>Pn</b> , <b>Pb</b> > Hp
Inter. phalanx	Mt < Ss, Mg < <b>Pn</b> , <b>Pb</b> > Hp	Mt < Ss, Mg < <b>Pn</b> , <b>Pb</b> ≈ Hp	Mt ≈ Ss, Mg < <b>Pn</b> , <b>Pb</b> ≈ Hp
Distal section (75%–100% bone length)			
Calcaneum	Mt ≈ Ss, Mg < <b>Pn</b> , <b>Pb</b> ≈ Hp	<b>Mt</b> > Ss, Mg < <b>Pn</b> , <b>Pb</b> > Hp	<b>Mt</b> > Ss, Mg < <b>Pn</b> , <b>Pb</b> > Hp
Fourth metatarsal	Mt < Ss, Mg < <b>Pn</b> , <b>Pb</b> > Hp	<b>Mt</b> > Ss, Mg < <b>Pn</b> , <b>Pb</b> < <b>Hp</b>	Mt ≈ Ss, Mg < <b>Pn</b> , <b>Pb</b> > Hp
Prox. phalanx	Mt < Ss, Mg < <b>Pn</b> , <b>Pb</b> > Hp	<b>Mt</b> > Ss, <b>Mg</b> > Pn, <b>Pb</b> < <b>Hp</b>	Mt ≈ Ss, Mg < <b>Pn</b> , <b>Pb</b> ≈ Hp
Inter. phalanx	Mt < Ss, Mg < <b>Pn</b> , <b>Pb</b> > Hp	Mt < Ss, Mg < <b>Pn</b> , <b>Pb</b> < <b>Hp</b>	Mt < Ss, Mg < <b>Pn</b> , <b>Pb</b> ≈ Hp

Note: Bolded values = a greater than 10% difference. See Table S3 for further detail.

Abbreviations: Hp, *Hadronomas puckeridgei*; Mg, *Macropus giganteus*; Mt, *Macropus cf. M. titan*; Pb, *Protemnodon brehus*; Pn, *Procoptodon browneorum*; Ss, *Sthenurus stirlingi*.

indicate where the slice of interest was located. The percentage bone length at the area of interest was noted and screenshots were taken at this point for all study species in BoneJ.

## 2.5 | Body size estimation

We estimated the body masses of the individual specimens studied here using a log–log regression of known body masses and pedal bone measurements for 64 extant macropodoid taxa and then extrapolating mass estimations from the same anatomical measurements in extinct taxa (or in our extant specimens of unknown individual body mass). The estimated body masses of the taxa used in this study are shown in Table 1; further details, and some body mass estimates for other extinct macropodiforms, plus details of the methodology and specimens, used are provided in the Data S1.

We considered it important to have individual mass estimates, rather than general species level ones (as in Helgen et al., 2006) because, even though we did perform size corrections on the data, we were still concerned about the effects of allometry, which we overcame in part by comparing pairs of sthenurines and macropodines of similar sizes (described below). In addition, as extant large kangaroos are highly sexually dimorphic, and we did not know the sex of our specimens (even the extant ones), it was important to determine a more precise individual estimation. For the purposes of this study, it is more important to confirm that the pairs of species compared are of similar size, rather than to know their body mass with a high degree of accuracy (although we note that the masses predicted for our extant sample specimens of *M. giganteus* and *O. rufus* are certainly within the range of known body sizes).

Previous studies of body mass reconstruction in extinct kangaroos have used extrapolations based on craniodontal metrics (e.g., Flannery, 1980; Murray, 1991) or from femoral circumference measurements (e.g., Helgen et al., 2006): each method comes with its own issues. Helgen et al. (2006) noted that cranial metrics are constrained by feeding requirements, and indeed sthenurine and macropodine dentitions differ due to their divergent specialized diets (Mitchell & Wroe, 2019; Wells & Tedford, 1995): they proposed femoral circumference as a more appropriate extrapolation, as load-bearing long bones show similar scaling relationships across unrelated taxa (Anderson et al., 1985; Anyonge, 1993; Reynolds, 2002).

Body mass estimation of taxa with no modern analog, such as the sthenurines and *Protemnodon*, and of species, which exceed the size of their extant relatives (as with these “giant” kangaroos), are always problematic. Each method and extrapolation from anatomical correlations has their own issues. The estimates calculated by Helgen et al. (2006), based on the femoral circumference, were made with two assumptions: that all kangaroos were hopping, and that there is similar isometric scaling in the long bones of sthenurines and macropodines. At the very least, the assumption regarding hopping may be false, which might suggest different scaling relationships, and therefore it is worth revising these extrapolations.

## 3 | RESULTS

### 3.1 | Second moment of area plots of resistances

Below we discuss in detail the second moment of area resistances for each bone: we describe the differences between cranio-caudal and medio-lateral resistances, but do not specifically describe the torsional resistances (although they are figured) as these represent the sum of the two bending axes. We compare the results by assigning the macropodines and the sthenurines to three different size classes: “large” (*Macropus* cf. *M. titan* [~176 kg] and *S. stirlingi* [~165 kg], “medium-sized” (*P. brehus* [~97 kg] and *H. puckridgi* [~73 kg], and “small” (*M. giganteus* and *P. browneorum* [both ~53 kg]). The “large” and “small” groupings represent pairs of related species, so they are first compared with each other in the descriptions below, and then the medium-sized pairing of more “wild card” taxa is considered. Note that this latter pair of species is termed “wild-card” because they are not typical for their subfamily: as previously mentioned, *P. brehus* is a large, derived Pleistocene macropodine that may have favored quadrupedal locomotion over hopping, and *H. puckridgi* is a smallish (for a sthenurine) and relatively basal late Miocene sthenurine that, unlike the Plio-Pleistocene taxa, retained a complete fifth pedal digit. Thus, unlike the other taxa considered, they do not constitute a “matching pair” in any other attribute except size: nevertheless, we consider them to be interesting inclusions.

Note that while the data have been adjusted to remove the effects of size, the effect of allometry remains: the large species (*M.* cf. *M. titan* and *S. stirlingi*) consistently show greater resistances than the small ones (*M. giganteus* and *P. browneorum*); the medium-sized species (*P. brehus* and *H. puckridgi*) usually show intermediate levels of resistance, but their patterns may be variable, especially that of *P. brehus*. Here, we will focus on comparisons between the pairs of similarly sized species, especially the species of *Macropus* and the monodactyl sthenurines (*Sthenurus* and *Procoptodon*).

The figures for the comparisons of the six species (Figures 3 and 5) show the comparison between each pair of resistance to bending along the bone, whether this is overall greater in the macropodine or the sthenurine, or equal in both, as determined by a greater than 10% difference in the average second moment of area values. Tables 2 and Table S3 show this information in more detail, and also show the differences in the proximal (first 25%), midshaft (middle 50%), and distal (last 25%) sections of the bones, as discussed in the text below.

#### 3.1.1 | Calcaneum

All species show peaks in resistance to cranio-caudal (CC) and medio-lateral (ML) bending at the proximal end (at around 25% bone length) and at the distal end (80%–90% bone length), with the distal peak being smaller than the proximal one. The proximal peak in all species is not at the very base of the calcaneum, in contrast to the pattern with the proximal peak seen in the other bones, but at around 25% of



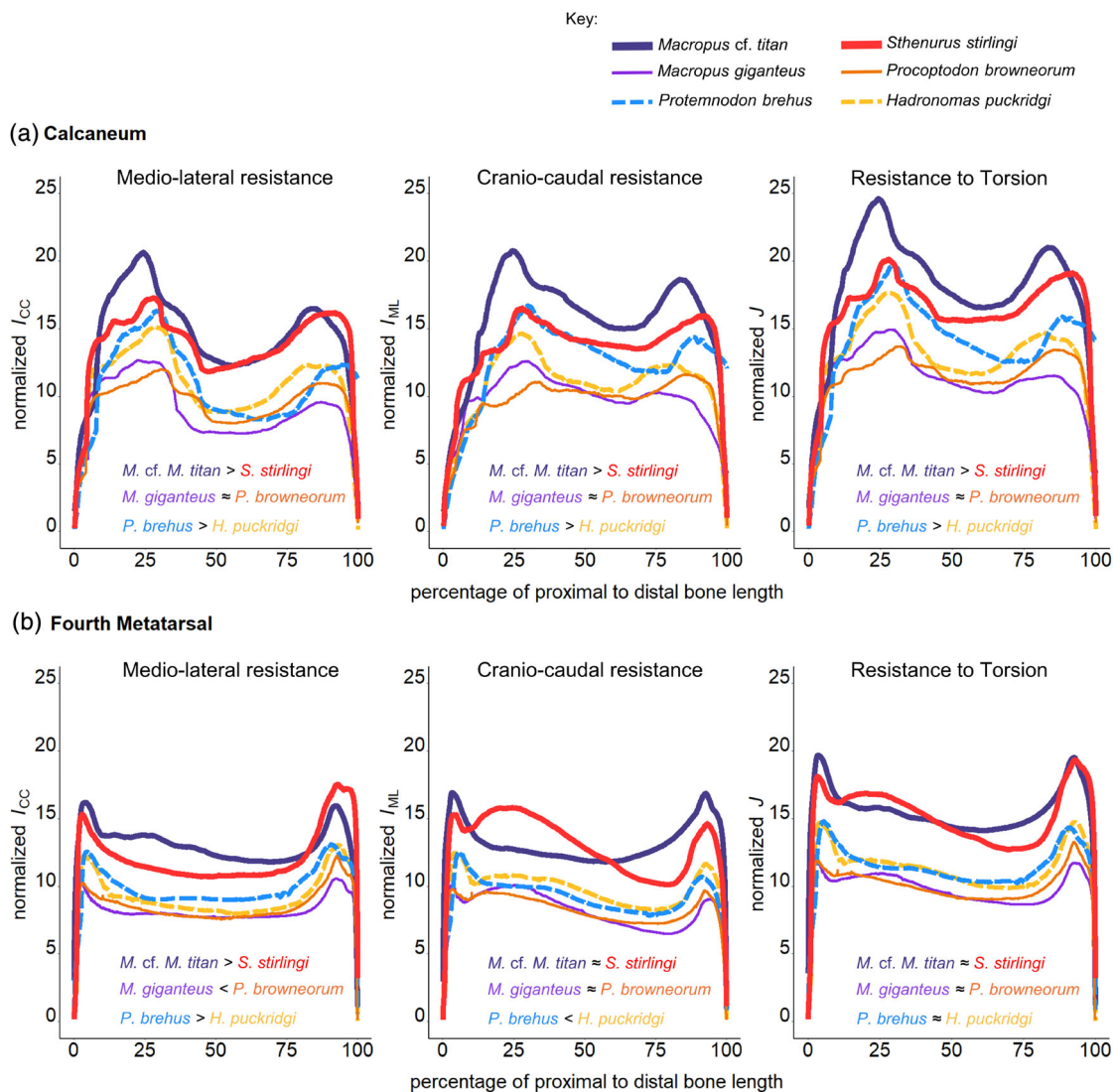


**FIGURE 3** Second moment of area analysis of resistance to bending along the length of the bones, adjusted for size by the fourth root (see methods section). Cool colors = macropodines; warm colors = sthenurines; thick lines = large taxa; thin lines = small taxa; dotted lines = intermediate-sized taxa. From left to right—Second moment of area around the cranio-caudal ( $I_{CC}$ ) axis, that is, resistance to medio-lateral bending; second moment of area around the medio-lateral ( $I_{ML}$ ) axis, that is, resistance to cranio-caudal bending; resistance to torsion ( $J$ ) (sum of CC and ML stresses). (a) Calcaneum; (b) fourth metatarsal. See Table 1 for details of taxa studied

bone length; this is approximately the position of the articular facets for the astragalus, through which the body weight is transmitted via the articulation with the tibia. (A small percentage of weight is directly transmitted slightly distally to this point via the contact with the fibula; Figure 3a).

The magnitude of resistances similar in both bending directions, although the midshaft resistances to ML bending tend to be a little lower than are the ones to CC bending, and the proximal and distal peaks of resistance are proportionally greater than the midshaft resistance (as is true in general for long bones, see Doube et al., 2018; McHorse et al., 2017; Figure 3a).

*M cf. M. titan* and *S. stirlingi*: the macropodine consistently shows higher levels of resistance in both bending axes, especially to CC bending, although the resistances to ML bending are equal at the distal end (Table 2, Table S3); here, there is slight difference in the

resistance profiles, with the distal peak for *M. cf. M. titan* coming slightly before the end of the bone, while that for *S. stirlingi* comes at the very tip of the bone. *S. stirlingi* has a somewhat different pattern of resistance to ML bending to *M. cf. M. titan*; the proximal and distal peaks are of similar size, in contrast to the higher proximal peak in *M. cf. M. titan*.

*M. giganteus* and *P. browneorum*: for both CC and ML bending, the macropodine has slightly higher resistances in the proximal peak, and the sthenurine has more equal (ML) or slightly higher (CC) resistances in the distal peak. The summed values of resistances over the whole bone are similar for the macropodine and the sthenurine, but *M. giganteus* is more resistant to bending in all directions than *P. browneorum* at the proximal end of the calcaneum, while *P. browneorum* is more resistant than the distal end (Table 2, Table S3).

*P. brehus* and *H. puckridgi*: The magnitude of the resistances tends to be more similar to those of the large species pair, especially for those in the proximal portion of the bone. The macropodine has the greater resistances along all portions of the bone except for the resistance to ML bending at the distal end, where the resistances are similar in both species (Table 2, Table S3). The resistances in both directions at the proximal peak for both taxa approach those of *S. stirlingi*, but not at the distal end, although distally *P. brehus* has markedly higher resistances to CC bending than *H. puckridgi*, especially along the midshaft of the bone.

### 3.1.2 | Fourth metatarsal

All species show peaks in resistance to bending at the proximal end (between 0% and 10% bone length) and at the distal end (80%–95%

bone length), usually with similar resistances at both ends. The magnitudes of resistance to both CC and ML bending are similar (Figure 3b).

*M. cf. M. titan* and *S. stirlingi*: the initial proximal peaks of resistance to bending in both directions are of similar magnitude; however, in the entire proximal portion and the midshaft *M. cf. M. titan* is more resistant to ML bending (with little decline in resistance along the midshaft from the proximal peak), while *S. stirlingi* is more resistant to CC bending, reflecting the second, more drawn-out peak in resistance with a maximum at around 25% of bone length. The situation is reversed in the distal end of the bone, where *S. stirlingi* is more resistant to ML bending, but *M. cf. M. titan* is more resistant to CC bending (Table 2, Table S3).

*M. giganteus* and *P. browneorum*: this small macropodine/sthenurine pair echoes the large one, where the proximal peaks of resistance are of a similar magnitude in both bending directions but the distal peak of resistance to ML bending is higher in the

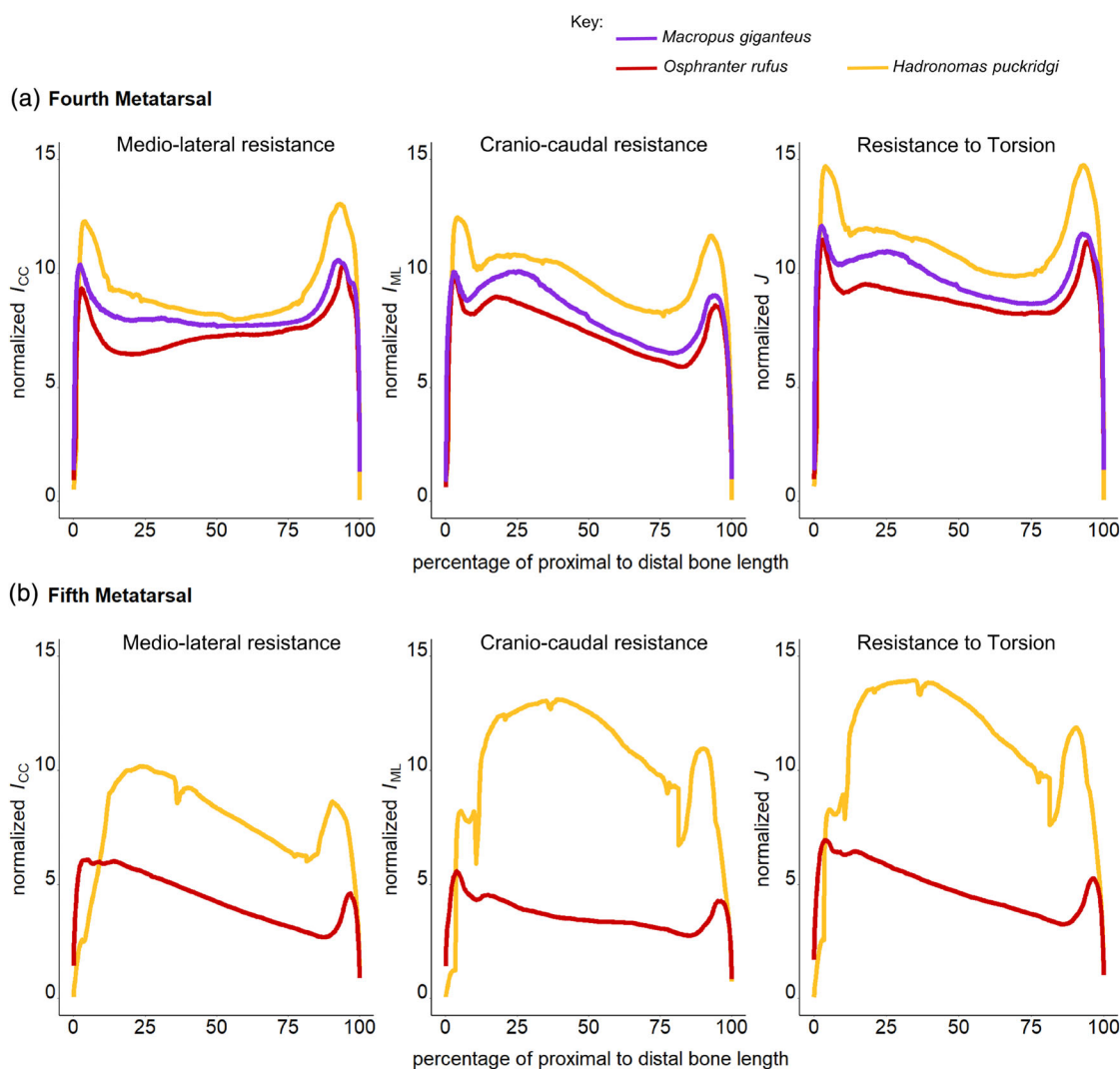


**FIGURE 4** Second moment of area analysis of resistance to bending along the length of the bones, adjusted for size by the fourth root (see methods section). From left to right—Second moment of area around the cranio-caudal ( $I_{CC}$ ) axis, that is, resistance to medio-lateral bending; second moment of area around the medio-lateral ( $I_{ML}$ ) axis, that is, resistance to cranio-caudal bending; resistance to torsion ( $J$ ) (sum of CC and ML stresses). For the (a) fourth metatarsal; (b) fifth metatarsals. See Table 1 for details of taxa studied

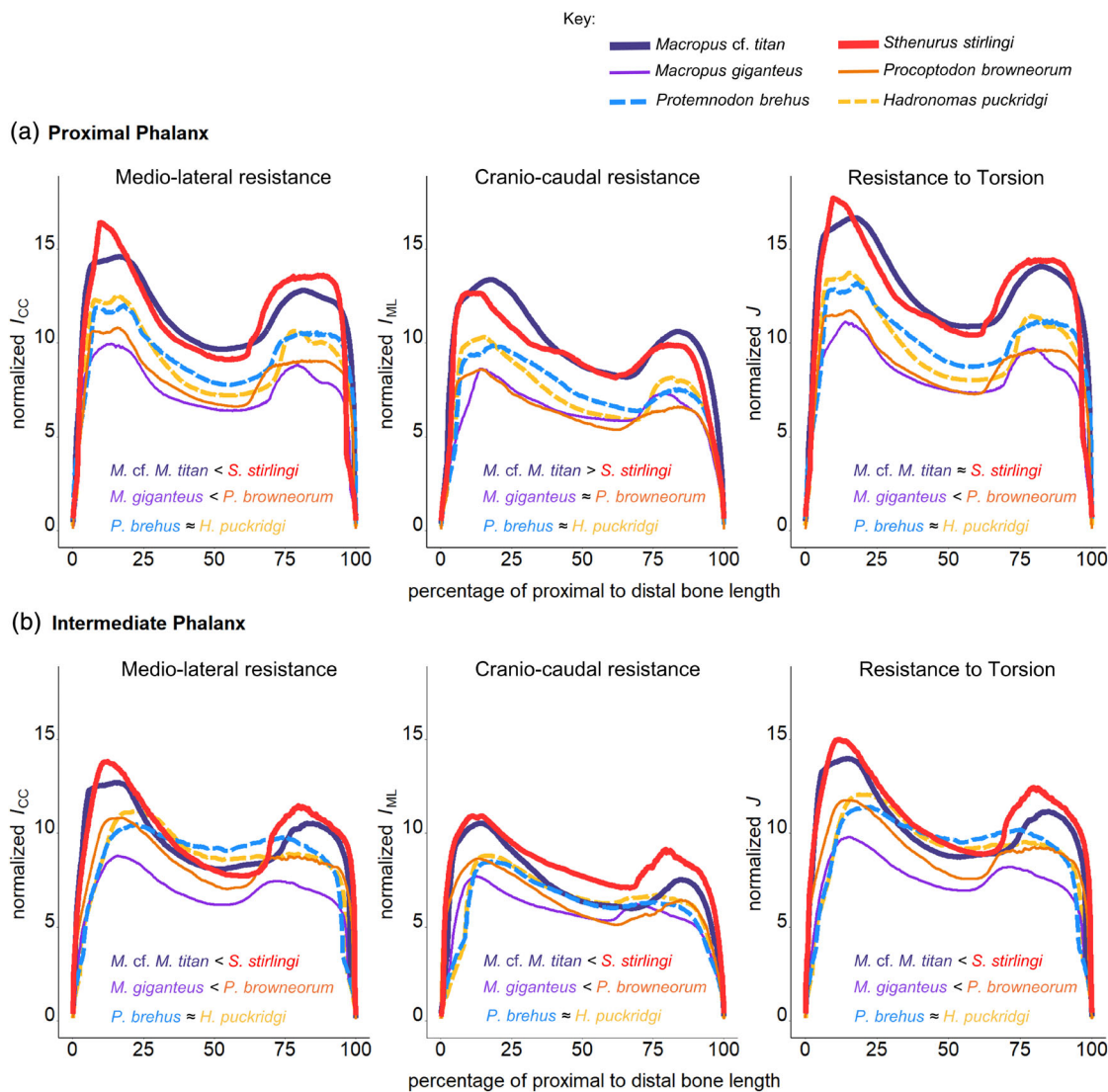


**FIGURE 5** Second moment of area analysis of resistance to bending along the length of the bones, adjusted for size by the fourth root (see methods section). Cool colors = macropodines; warm colors = sthenurines; thick lines = large taxa; thin lines = small taxa; dotted lines = intermediate-sized taxa. From left to right—Second moment of area around the cranio-caudal ( $I_{CC}$ ) axis, that is, resistance to medio-lateral bending; second moment of area around the medio-lateral ( $I_{ML}$ ) axis, that is, resistance to cranio-caudal bending; resistance to torsion ( $J$ ) (sum of CC and ML stresses). (a) Proximal fourth pedal phalanx; (b) intermediate fourth pedal phalanx. See Table 1 for details of taxa studied

sthenurine. However, unlike the condition in the larger species pair, the resistance to CC bending in the proximal part of the bone is greater in the macropodine, while the resistance to ML bending is greater in the sthenurine, and the resistance in the distal part of the bone is greater in the sthenurine in both bending directions (Table 2, Table S3).

*P. brehus* and *H. puckridgi*: The magnitude of the resistances are more similar to those of the small species pair, but the pattern of the resistances in both axes is more similar to the large species than to the small ones in the proximal part and midshaft portions of the bone; in the distal portion of the bone *P. brehus* is unique for a macropodine in having a greater ML resistance than the sthenurine, although these species resemble the small pair in the sthenurine having a greater distal CC resistance than the macropodine (Table 2, Table S3).

### 3.1.3 | Fifth metatarsal

The fifth metatarsal was not available for *M. cf. M. titan*. In the case of *P. brehus*, only the fourth metatarsal was analyzed, although the fifth digit in this taxon is considerably more robust than in *Macropus*. However, we did make a comparison of both fourth and fifth metatarsals between the basal sthenurine *H. puckridgi* and a different large extant macropodine to the one used in the rest this study, *O. rufus* (the red kangaroo, likely a female individual, estimated body mass ~36 kg), here shown in comparison with the results for the fourth metatarsal for *M. giganteus* (Figure 4).

Although the Plio-Pleistocene sthenurines have lost the fifth digit, the fifth metatarsal of *H. puckridgi* is a robust bone (see Murray, 1995), comparatively much more robust than the condition in large species of

*Macropus* and *Osphranter*. A note of caution in the comparisons below: the two metatarsals (i.e., fourth and fifth) of *O. rufus* belong to the same individual while those of *H. puckridgi* belong to different individuals, although ones of a similar size.

Figure 4a compares the second moment of area resistances in the fourth metatarsal of *H. puckridgi* and *O. rufus*, and shows them to be similar, although of slightly greater magnitude in the sthenurine, which is to be expected given its larger size (~73 vs. ~36 kg). The magnitudes of resistances are similar in the two macropodine species, although *M. giganteus* shows greater resistances in the proximal part of the bone (although not in size of the proximal peak). *H. puckridgi* also shows especially greater resistance to CC bending in the proximal part of the bone, likely following the area of cranio-caudal cortical thickening, as discussed above for *S. stirlingi*. However, there are marked differences in the resistance in fifth metatarsal (Figure 4b): the magnitude of resistances in the fifth metatarsal of *O. rufus* are around half of those in the fourth metatarsal, but they are much greater in *H. puckridgi*; here the ML resistances are of similar magnitude (but a little lower) to those in the fourth metatarsal, and actually greater than in the fourth metatarsal to CC bending. The patterns of resistance are also different: in their resistances to ML bending both taxa show a proximal peak, a slow decline along the length of the bone and then a (much smaller) distal peak; *O. rufus* shows a similar pattern to CC bending, but *H. puckridgi* shows a small proximal peak, followed by a rise to a much larger resistance persisting between around 15%–18% of bone length, followed by a distal peak that is larger than the initial proximal one.

### 3.1.4 | Proximal phalanx

The resistances are higher to medio-lateral bending than to cranio-caudal bending in all species. All species show a similar pattern of resistances in both bending planes: after an initial proximal peak at between 10% and 15% of bone length, resistances fall until around 60% of bone length, at which point they start to rise to a distal peak that is smaller than the proximal one, peaking at around 80% of bone length. The distal peak in ML resistance is more prolonged and hence squarer in shape than the peak in CC resistance (Figure 5a).

*M. cf. M. titan* and *S. stirlingi*: Overall the macropodine is more resistant to CC bending and the sthenurine to ML bending; in both instances, these differences are more pronounced at the proximal and distal ends, while the midshaft resistances are more similar (Table 2, Table S3).

*M. giganteus* and *P. browneorum*: a similar pattern of resistances to ML is present in the smallest pair of taxa, although the resistances to CC bending of the phalanx are more equal and, unlike the condition in the large pair, the sthenurine is the more resistant to CC bending in the proximal phalanx (Table 2, Table S3).

*P. brehus* and *H. puckridgi*: The magnitude of resistances is more similar to those of the small species pair, but the pattern of resistances in the midsized species pair is a little more variable than in the other two pairs. Here the sthenurine, *H. puckridgi*, is more macropodine-like

in being in general the more resistant species to cranio-caudal bending (except for the CC resistance the midshaft portion; Table 2, Table S3).

### 3.1.5 | Intermediate phalanx

The overall magnitudes and patterns of resistances in the intermediate phalanx are similar to, but a little lower, to those in the proximal phalanx, with the exception of *P. brehus* that shows some unique features. See Figure 5b.

*M. cf. M. titan* and *S. stirlingi*: the sthenurine is more resistant than the macropodine along the entire length of the bone, in both bending directions. As with the proximal phalanx, the ML resistance for the distal end is more prolonged in the sthenurine, with the peak starting at around 70% of the bone, preceding the macropodine rise (Table 2, S3).

*M. giganteus* and *P. browneorum*: bending resistances in the sthenurine are markedly higher along the entire length of the bone than the macropodine, especially in the ML direction; both species have rather prolonged resistances at the distal end (Table 2, S3).

*P. brehus* and *H. puckridgi*: both species have rather different patterns of resistances to the other macropods. Both have similar resistances to CC bending, but with the ML resistances the sthenurine is the more resistant in the proximal portion of the bone, but *P. brehus* tends to be the more resistant, especially along the midshaft, in the other portions of the bone (Table 2). The ML resistance pattern in *P. brehus* is unlike that of the other macropods; the proximal peak is at around 20% of bone length, with very little drop in resistance until a distal peak at around 75% of bone length, which is followed by only a slight drop until the “fall off” at around 90% of bone length as seen in the other taxa (Table 2, S3).

## 3.2 | Bone distribution

As bones with thicker cortices experience lower stress for the same applied load, variation in the cross-sectional morphology likely demonstrates differences in the distribution of stress during locomotion. This may provide an insight into patterns of weight-bearing and can therefore be utilized to hypothesize locomotor mode. This variation is not recorded using more quantitative methods; thus, we here present a simple comparative study of the osteological geometry.

### 3.2.1 | Calcanea

The cross-sections of the calcanea, taken at 84% of the bone length, are shown in Figure 6. This percentage of proximal to distal bone length equates to near the top of the calcaneal tuber, just proximal to (i.e., below) the epiphysis.

The macropodine calcanea are all cone-shaped, deeper (in the cranio-caudal direction) than wide, and with a relatively pointed cranial apex. In at least the *Macropus* species, there is evidence of

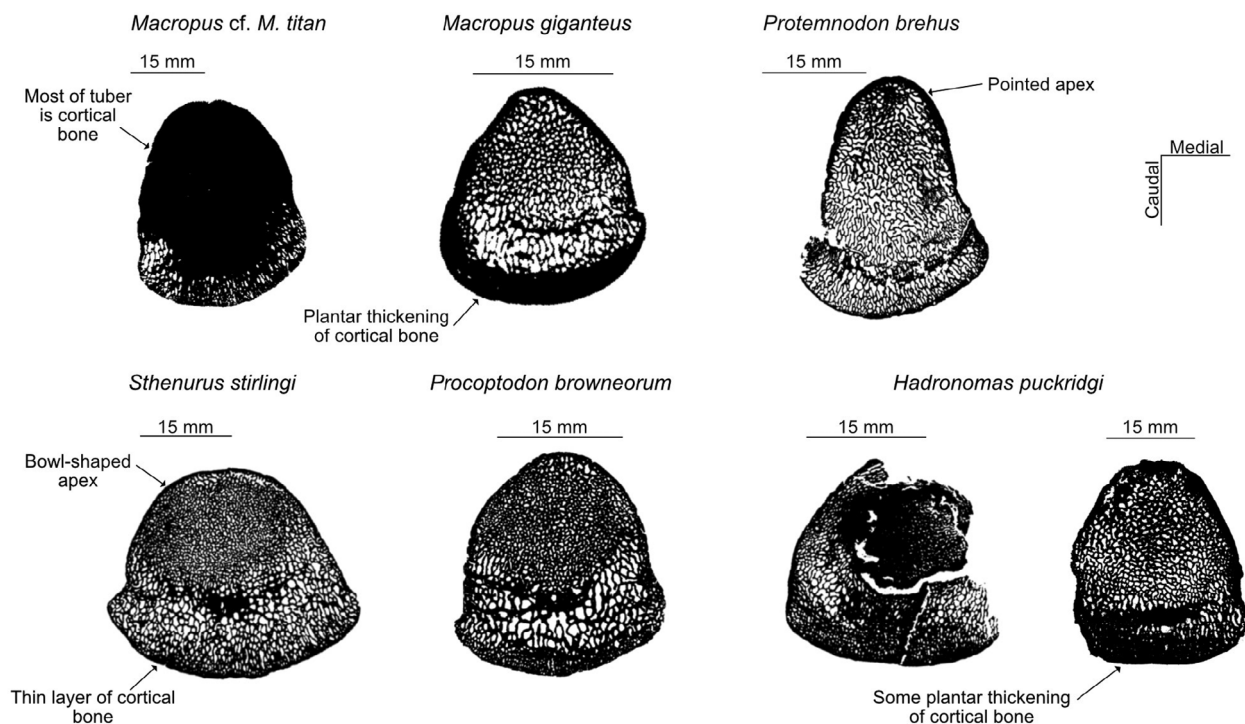


**FIGURE 6** Cross-sections of left calcanea, at 84% of the bone length, seen in proximal projection (*M. cf. M. titan* is reversed). Two calcanea are shown for *H. puckeridgei*: The left-hand one shows a complete but slightly damaged specimen (NTM P9336, the specimen used in the SMOA analysis) where it was possible to ascertain the precise level of the cross-section; the right hand one (NTM P10115, reversed) is from an isolated tuber, where the level of cross-section cannot be precisely ascertained, but it was taken at approximately the same level (i.e., just below the epiphysis) and provides a better image of the internal anatomy. See Table 1 for details of taxa studied

considerable thickening of cortical bone, most notably on the plantar (caudal) surface as well as the cranial one. The sthenurine calcanea are general more bowl-shaped, as wide or wider than deep, without evidence of extensive cortical thickening at the point of the cross-section, and there is never evidence of plantar cortical thickening. In external view, the sthenurine calcaneal tuber appears broadened compared to that of the macropodines (Figure 2), so the relatively lesser extent of cortical thickening is of note.

*M. giganteus* exhibits a thickened border of cortical bone, which is particularly pronounced on the cranial and plantar surfaces. The plantar thickening is present throughout the length of the calcaneal tuber, while the cranial thickening is present only at the more distal end of the tuber, and decreases again at the very tip of the tuber.

*M. cf. M. titan* lacks the thick layer of plantar cortical bone seen in *M. giganteus*, but this absence may be because the plantar surface of the entire tuber exhibits some taphonomic abrasion. The cranial thickening in *M. cf. M. titan* is more extensive than that in *M. giganteus*—continuing until the distal tip of the calcaneal tuber: almost the entire distal tuber is comprised of cortical bone, with only a narrow more plantar region of trabecular bone.

The calcaneal tuber of *P. brehus* is deeper and narrower than in the *Macropus* species, and lacks any degree of cortical thickening at the point of the cross-section. More proximally on the tuber there is a degree of cranial thickening, but there is never any evidence of plantar thickening.

Although the calcaneum of *S. stirlingi* exhibits cranial thickening of the cortical surface, extending from the proximal end of the tuber up to its distal broadening, by the point of the cross-section there is only a thin border of cortical bone that is relatively evenly distributed around the outer surface of the tuber. *P. browneorum* exhibits a nearly identical pattern of distribution of cortical bone to *S. stirlingi*; however, the calcaneal tuber appears relatively narrower than that of *S. stirlingi* externally, probably a morphology related to its smaller size.

The calcaneum of *H. puckeridgei* appears somewhat intermediate in shape between the macropodine and sthenurine conditions. It is a little more cone-shaped than in the other sthenurines examined here, and has a moderate thickening of cortical bone on the cranial surface, but lacks a *Macropus*-like plantar layer of thicker cortical bone (although there is perhaps a little more extensive plantar thickening than in the other sthenurines).

### 3.2.2 | Metatarsals

The cross-sections of the fourth metatarsals, taken at 23% of the bone length, are shown in Figure 7. This percentage of proximal to distal bone length equates around a quarter of the length of the bone distal to the articulation with the tarsus, and captures the area of cranio-medial thickening seen in *S. stirlingi*.

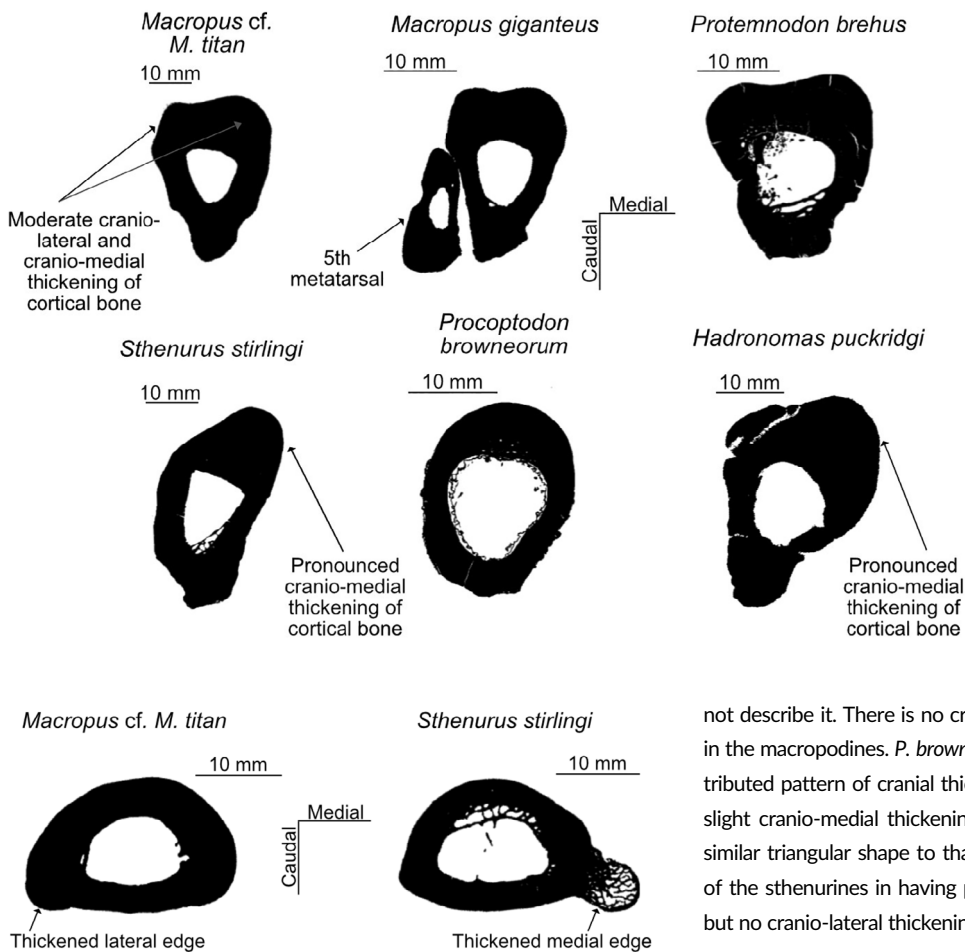


**FIGURE 7** Cross-sections of left fourth metatarsals, at 23% of the bone length, seen in proximal projection (*M. cf. M. titan* and *H. puckeridgei* are reversed). Note that the fifth metatarsal is included in the section for *M. giganteus*: This bone is reduced to a proximal splint in *Sthenurus* and *Procoptodon* but is present in the other taxa, although not shown here. See Table 1 for details of taxa studied

**FIGURE 8** Cross-sections of left proximal fourth pedal phalanges, at 64% of the bone length, seen in proximal projection (*M. cf. M. titan* is reversed). See Table 1 for details of taxa studied

The cross-sections of *M. giganteus* and *Macropus cf. M. titan* demonstrate similarities in the distribution of the bone—the shaft of the bone is triangular (with the apex on the plantar side) with a degree of cranial thickening on both lateral and medial aspects but slightly more so medially (but not to the extent seen in *S. stirlingi*, see below). It can be seen in *M. giganteus* that the fifth metatarsal cross-sectional shape is somewhat of a mirror image of the fourth metatarsal, with a cranial apex and broadened plantar edge, with pronounced lateral thickening. (A fifth metatarsal would have also been present in the other macropodines, and in *H. puckeridgei*.) *P. brehus* exhibits a somewhat similar cross-sectional morphology not dissimilar to that of the *Macropus* species. Thickening of cortical bone is present on the cranial and plantar sides, but the cranial edge is broader than in *Macropus*, and the plantar edge of the bone has a broader and blunter taper. The fifth metatarsal (not shown) is relatively much more robust than in *Macropus*, and also somewhat divergent from the fourth one.

*S. stirlingi* exhibits medial thickening of the cranial side of the metatarsal from 7% to 64% of the bone length and this can be observed as a profound medial bulge in the cross-section of the bone. This thickened ridge is figured in Wells and Tedford (1995, figure 35, p. 73) but they do

not describe it. There is no cranio-lateral thickening, unlike the condition in the macropodines. *P. browneorum* exhibits a generally more evenly distributed pattern of cranial thickening than is seen in *S. stirlingi*, with only slight cranio-medial thickening. The calcaneum of *H. puckeridgei* shows a similar triangular shape to that of the macropodines, but resembles that of the sthenurines in having prominent cranio-medial cortical thickening but no cranio-lateral thickening.

### 3.2.3 | Proximal phalanges

The cross-sections of the fourth metatarsals, taken at 64% of the bone length, are shown in Figure 8. Only *M. cf. M. titan* and *S. stirlingi* were examined here. The critical issue at this level of the bone length is that the lateral edge is thickened in the macropodine while the medial edge of the phalanx is thickened in the sthenurine. Some lateral thickening occurs more distally in the phalanx of *S. stirlingi*, but the medial thickening is always more prominent; the converse is true for *M. cf. M. titan*.

## 4 | DISCUSSION

### 4.1 | Resistance to bending

While all of the study species exhibit resistance peaks at the articular ends and a resistance trough in the midsection for every bone, the position along the bone and percentage of the bone length of the resistance peaks varies between species, reflecting their diverse anatomies. The larger study species (*M. cf. M. titan* and *S. stirlingi*) exhibit consistently higher resistances than the other species, which is expected as despite the corrections for body size some allometric effects remain.

In the calcaneum (Figure 3a) macropodines, in general, have higher resistance to bending than the sthenurines, especially at the proximal end (i.e., at the calcaneal head). Higher values in the proximal part of the bone than the distal part in all species likely reflect the fact that only the proximal part of the bone is a load-bearing surface (although the distal portion of the bone has to resist the action of the Achilles tendon). The macropodines are particularly resistant to cranio-caudal bending, especially at the proximal end of the bone, but the monodactyl sthenurines may show greater resistance at the distal end, especially to medio-lateral bending. This difference likely reflects the expanded tip of the calcaneal tuber in these sthenurines (Figure 2).

In the fourth metatarsal (Figure 3b), for the pairs of *Macropus* species and monodactyl sthenurines, *S. stirlingi* is unique in its large second peak of proximal resistance to cranio-caudal bending (reflecting the cranio-medial thickening of the proximal shaft seen in the cross-sections, Figure 7); this second peak is echoed slightly by *H. puckeridgei*, but not by *P. brownorum*. The patterns of resistance to bending are somewhat different between the three pairs of species; the only overall pattern is that the sthenurines are usually more resistant to bending (especially to mediolateral bending) than the macropodines in the distal portion of the bone.

Note that there is a slight difference in the pattern of resistances to bending in the fourth metatarsal between *M. giganteus* and *O. rufus*, although the overall magnitudes are similar (Figure 4). It is not clear if this reflects individual differences, species differences, or perhaps most likely, sexual differences: the *M. giganteus* specimen is likely a male, and the *O. rufus* specimen likely a female, and large male kangaroos spend more time on their hind legs in non-locomotor activities (e.g., fighting) than do females (Dawson, 1983).

There is little information in the current literature about the supportive or weight-bearing role played by the fifth digit in kangaroo locomotion. A prior study (Wagstaffe, 2018) showed that the fourth metatarsal bending resistance of *M. giganteus* was increased by around 25% if the fourth and fifth metatarsals were considered together. The differences between the resistances in the fifth metatarsal in *O. rufus* and *H. puckeridgei* are intriguing, and indicative of a greater capacity for load-bearing by this bone in the sthenurine than in the macropodine (although note that Murray, 1995 considered that *H. puckeridgei* did not bear any weight on the fifth digit). The reasons for the loss of the fifth digit in derived sthenurines are enigmatic. Janis et al. (2014) proposed that this loss did not represent a functional change, but instead was an epigenetic byproduct of a developmental shift in the evolution of the sthenurine hand, where the fifth digit has been greatly reduced as the second, third, and fourth ones have been elongated. This hypothesis could be tested by the looking at the manual digits of *H. puckeridgei*, but unfortunately, its hand is still unknown.

The bending resistances of the fifth metatarsals are likely greater in other macropodines, where the bone is more robust than in the *Macropus* complex species; the fifth metatarsal is more robust in more basal macropodines such as pademelons (*Thylogale* spp.) and the quokka (*Setonix brachyurus*), and especially so in species of tree-kangaroos (*Dendrolagus*, see Prideaux & Warburton, 2010b), and also in *Protemnodon*.

In the proximal phalanx (Figure 5a), the monodactyl sthenurines tend to be more resistant to medio-lateral bending than their macropodine pair at both proximal and distal ends. The pattern in the mid-sized species pair is a little more variable; here the sthenurine, *H. puckeridgei*, is more macropodine-like in being in general the more resistant one to cranio-caudal bending. This may reflect the fact that, like the macropodines, *H. puckeridgei* retains the fifth digit that would play a load-bearing role. In the intermediate phalanx (Figure 5b) the *Macropus* species/monodactyl sthenurine pairs show similar patterns of resistance, with the sthenurines having greater magnitudes of resistance in all sections of the bone in both bending axes. The profile for the midshaft resistance to medio-lateral bending in *P. brehus* is distinctly different from all the other taxa, with little drop in resistance between the proximal and distal peaks. *Protemnodon* species have intermediate pedal phalanges (on both fourth and fifth digits) that are exceptionally short and broad (Wagstaffe, 2018), which may account for the difference in this species from the other macropods.

In summary, while the differences in patterns of bone resistance do reflect the phylogenetic groupings to a certain extent, the differences between *P. brehus* and the closely related *Macropus* species, and the resemblance of *H. puckeridgei* to the macropodines in certain instances, indicates that these differences are likely to reflect function rather than phylogeny. While these bone resistances cannot be used to determine the mode of locomotion, they do support the hypothesis that macropodines and sthenurines were experiencing different kinds of locomotor stresses, and hence were likely to have different types of locomotion. The difference of *P. brehus* from the *Macropus* species also indicates that its mode of locomotion was dissimilar: as previously mentioned, other authors have inferred that large species of *Protemnodon* were primarily quadrupedal (Den Boer, 2018; Jones, 2020—a conclusion also reached by Kear et al., 2008 for the smaller species of the genus).

## 4.2 | Bone distribution

The results of the osteological cross-sections are of interest as they provide insight into the internal structural differences of the bones of the study species. Of particular note, is the difference between the external and internal anatomy of *Macropus* compared to the sthenurines. Despite the gracile external appearance of the bones of *Macropus* species, the cross-sections of the calcanea and metatarsals of *M. giganteus* and *M. cf. M. titan* reveal extensive thickening of the cortical bone, which allows these species to resist bending stresses that are generally equal to or greater than those of robust sthenurine species of similar body size. Instead, in the sthenurines, the broadened appearance of at least the articular ends is a result of enlarging the entire portion of that bone, as opposed to thickening of the cortical bone within the bone.

The general robusticity and broadening of the sthenurine bones compared to *Macropus* has previously been suggested as an adaptation for a different locomotive mode to the bipedal hopping of *Macropus*. Janis et al. (2014) proposed that the robusticity of the sthenurine

hind limb (and indeed, other bones of the postcrania such as the pelvis and the lumbar vertebrae are also particularly robust) might be an adaptation to allow each of the limbs to individually support the full weight of the body during locomotion. During bipedal hopping, the limbs are used simultaneously and never individually support the full body weight of the animal. Conversely, in bipedal striding, each hindlimb alternates in individually supporting the full body weight of the animal, which may necessitate limbs of bipedal striders to withstand higher forces (although it is likely that such striding sthenurines would not have engaged in the high speeds seen in large extant hopping macropodines).

Doube et al. (2018) noted that, while in artiodactyls the tibia becomes relatively more robust with increases in body size, in macropods it becomes relatively less robust, showing increased gracility with increasing size, although the femur becomes more robust. Janis et al. (2014) showed similar trends, but noted that the scaling relationships differed if large extant *Macropus* (including *Osphranter*) were excluded from the analysis and the large extinct species were included: while the femur became relatively more robust in extant taxa, if the extinct ones were included the exponent was higher; likewise, with the inclusion of extant large taxa, tibial robusticity decreased with size, but no decline was observed if the extinct taxa were included. They concluded that the large extant kangaroo species are exceptionally gracile, and not typical of macropodids in general.

The differences in the bone distribution in the calcanea are of interest due to the role of the calcaneum as a site for tendon attachment (the Achilles tendon and, to a certain extent, the plantaris). Despite the cortical thickening in the *Macropus* spp., the overall shape of the tuber remains narrow, reflecting the attachment of a narrow Achilles tendon. As previously noted, for a given tendon volume, long and narrow tendons are the most effective at elastic energy recovery (Biewener, 2008); thus, in species that hop broadening of the tuber would be counterproductive, as it would then not be of a suitable shape for the attachment of a narrow Achilles tendon; but the tuber still needs to be resistant to the forces generated by the gastrocnemius muscle via the Achilles tendon. The extensive thickening of the cortical bone in the tuber of the *Macropus* spp. is likely an adaptation to locomotor stresses: these stresses would result both from the action of the gastrocnemius in retracting the foot for propulsion, and also by the need of the muscle and its tendon to balance torques (rotational forces) during the stance phase of hopping, where the calcaneal heel is the moment arm (“ $r$ ” in Biewener, 2005) for those torques. These locomotor issues will be intensified in a hopping animal because of the need to maintain a crouched posture during stance prior to take-off (see Bennett, 2000). A larger hopper will encounter even greater rotational forces because of the increased ground reaction force, and this explains why the extent of cortical bone is so much greater in *M. cf. M. titan* than in *M. giganteus*. Indeed, the morphology of the calcaneum in this taxon, as well as the similarity of the distribution of bone bending resistances, provide support for the notion that this animal, despite being “oversized” (according to McGowan, Skinner, & Biewener, 2008), was able to hop.

In contrast to macropodines, *S. stirlingi* exhibits a broadened calcaneal tuber (and limited cortical bone thickening) which may be indicative of attachment of a broad tendon. (Both a broad distal calcaneum and a short and broad Achilles tendon are evident in extant tree-kangaroos, *Dendrolagus* spp; Warbuton et al., 2012). A broad Achilles tendon would be less effective at restoring elastic energy, as is required for bipedal hopping, but would likely withstand the stresses that arise from the previously noted issues of scaling and tendon safety factor associated with large macropods. The smaller sthenurines *P. browneorum* and *H. puckeridgei* are also characterized by an absence of extensive cortical bone thickening, especially plantar thickening—although *H. puckeridgei* evidences some *Macropus*-like cranial thickening, while the overall shape of their tubers is somewhere in between the narrow tuber of *Macropus* spp. and the broadened tuber of *S. stirlingi*. If sthenurines engaged in bipedal striding, rather than hopping, then they would have been able to maintain a less crouched posture during locomotion; this in turn would also reduce rotational forces at the ankle joint during the stance phase, and would mean that the calcaneal tuber would not have to withstand such high resistances, and so would not require cortical bone thickening.

The calcaneal tuber of *P. brehus* is also narrow and long, but lacks the degree of cortical bone thickening observed in *M. giganteus* or *M. cf. M. titan*. This suggests that *P. brehus* maintained a macropodine type of narrow Achilles tendon attachment site but it was not subject to the same locomotive stresses as the *Macropus* species. This provides further evidence for the hypothesis of primarily quadrupedal locomotion in this taxon.

In hominids, the only extant striding bipedal mammals, the body weight is shifted onto the medial side of the leg during the stance phase: the anatomy of a robust, non-opposable, adducted hallux is considered to be key for human bipedalism, because it allows the individual to shift its weight medially while remaining balanced (and avoid toppling over laterally) while bearing weight on one leg at a time (Aiello & Dean, 1990; Harcourt-Smith & Aiello, 2004). Despite the differences in posture and hindlimb anatomy between macropods and hominids, the notion that a biped bearing weight on one foot at a time would be shifting its weight to the medial side can be used to generate a predictive hypothesis: is there any evidence in sthenurines (vs. macropodines) for limb bones that demonstrate medial strengthening? The distribution of cortical bone in the proximal phalanx, as seen in the cross-sections, shows a predominance of medial thickening in *S. stirlingi* versus slight lateral thickening in *M. cf. M. titan*. The fourth metatarsal of *S. stirlingi* shows an extensively thickened cranial ridge on the medial side on the proximal two-thirds of the bone: although this is not apparent in the much smaller sthenurine *P. browneorum*, a degree of medial thickening is seen in the somewhat larger *H. puckeridgei*. The macropodines show prominent medial and lateral thickenings on the cranial surface of the fourth metatarsal, the medial one being slightly larger: but these areas of thickening are nowhere near as extensive as in *S. stirlingi*, and they are not accompanied by a thickened ridge stretching for over two-thirds the length of the bone. This cranio-medial thickening in the macropodine fourth



metatarsal is offset by the presence of the plantar-lateral thickening in the fifth metatarsal (see Figure 7).

Thus, there is good evidence, from the internal structure of the bones, that at least the larger sthenurines, such as the ~160 kg *S. stirlingi*, had pedal bone anatomies consistent with the hypothesis that they were shifting their weight to the medial side of the limb during locomotion, which may be indicative of bipedal striding. The lesser indication of this anatomy in the smaller sthenurines, such as the ~50 kg *P. browneorum*, may simply be an effect of allometry, or may reflect a difference in locomotion. Both large and small monodactyl sthenurines have humeral anatomy indicative of reduced weight-bearing on the forelimbs (Janis et al., 2020; Jones, 2020; Jones et al., 2021), and likely used a bipedal striding as slow gait as an alternative to quadrupedal locomotion. However, only the larger sthenurines approached or exceeded the proposed weight limit for hopping, either 140 kg (McGowan, Skinner, & Biewener, 2008) or 160 kg (Snelling et al., 2017); *S. stirlingi* would likely have had severe problems with hopping (especially without the resistant calcaneal anatomy of *M. cf. M. titan*), whereas *P. browneorum* may have retained hopping as a fast gait, even though no sthenurine had the derived macropodine anatomy (e.g., as in the genus *Macropus*) adapted to rapid and sustained hopping at larger (>25 kg) body sizes (Janis et al., 2014).

### 4.3 | Other considerations about sthenurine/macropodine differences

Further evidence for the hind limbs of sthenurines bearing more weight during locomotion than in macropodines (implying unilateral hind limb weight-bearing) comes from the structure of the tarsus. Fusion of the distal tarsals to a greater or lesser extent, especially of the cuneiform bones, is common in ungulates (Howell, 1965) but is not seen in extant kangaroos. However, Wells and Tedford (1995, p. 66) noted that in at least the adults of sthenurines the tarsal cuneiform bones fuse into a single complex, and the proximal ends of the vestigial second and third metatarsals may also be involved in this fusion. Wells and Tedford (1995) attributed this difference between sthenurines and macropodines to the loss of weight-bearing by the fifth digit in sthenurines, with more weight now being transmitted through the medial side of the tarsus. We suggest that an additional reason for this fusion might be increased stresses on the tarsus in general during single-leg weight-bearing, especially on the medial side (see earlier discussion about medial side weight-bearing). We note that this fusion is unlikely to be simply due to the much larger size of sthenurines than extant macropodines, as fusion is not apparent in *M. ferragus*, an extinct species of similar size to *S. stirlingi* (see Data S2).

A further indication of increased stresses on the sthenurine foot lies in the form of the sesamoid ligaments. Tedford (1967) noted in *P. goliath* that the plantar surface of the proximal phalanx had proximal scars not only for the short sesamoid ligaments, as in *Macropus*, but also a distal extent of these scars, possibly

representing the oblique sesamoid ligaments seen in *Equus*, where they form a distinctive “V-scar” extending to around 70% the length of the bone (see Janis & Bernor, 2019). While *M. ferragus* and *S. stirlingi* have similarly sized proximal paired sesamoid bones (Figure S5), there is indeed a greater distal extent of the sesamoid ligament scars of *S. stirlingi* and other sthenurines, extending to around 50% of the length of the phalanx, and bearing some similarity to the equid V-scar. Tedford (1967) proposed that these elaborated sesamoid ligaments in sthenurines represented the possession of an equid-like “spring foot,” associated with increased cursoriality. However, we note that the equid “spring foot” involves pronounced flexion at the fetlock (metapodial/phalangeal) joint during locomotion in conjunction with an unguigrade foot posture, which was not the sthenurine condition. We propose that this evidence of more extensive sesamoid ligaments simply reflects increased stress on the sthenurine foot during unilateral weight-bearing locomotion (see also Janis et al., 2021).

## 5 | CONCLUSION

The gross anatomy of the limb bones of sthenurines and macropodines shows many differences, apart from the well-known generally more robust nature of sthenurines (e.g., Wells & Tedford, 1995), which have been interpreted as indicative of differences in locomotor behavior (Janis et al., 2014). The hypothesis of Janis et al. (2014) that sthenurines engaged in bipedal striding has gained support from a fossil trackway (Camens & Worthy, 2019). Here, we compare sthenurine and macropodine bone microanatomy to see if this hypothesis can be further supported. Differences in, say, patterns of stress resistance to bone bending may simply indicate differences in locomotor behavior, and not determine the nature of those differences. However, we consider that the results of the resistances to bending, in combination with the results of the cortical distribution of bone within the pedal long bones, do indeed provide strong evidence of sthenurines employing bipedal striding.

Differences between macropodines and sthenurines are apparent in the resistances to bending of pedal long bones, and distribution and amount of cortical bone within the bones, especially between the monodactyl sthenurines and the species of *Macropus*. In the calcaneum, macropodines not only show higher resistances to bending stresses (especially at the tip of the tuber) but, in contrast to sthenurines, have a distribution of cortical bone within the tuber indicative of a great deal of internal strengthening. The calcaneal tuber of a hopping mammal, especially a large one, must be especially resistant to torques (rotational forces) around the ankle during the stance phase of locomotion: this difference between macropodines and sthenurines certainly supports the hypothesis that sthenurines did not hop, or at least were not regular and rapid hoppers like extant *Macropus* species. In addition, the internal anatomy of the calcaneal tuber of *M. cf. M. titan*, which has extremely dense cortical bone, is a good indicator that it maintained the macropodine mode of hopping locomotion, despite its large size.

Sthenurines and macropodines differ in the bending resistances in the fourth metatarsal, sthenurines having greater resistance to medio-lateral bending. The two largest taxa are unique in different ways: the sthenurine, *S. stirlingi*, has a large and extended area of proximal resistance to cranio-caudal bending, while the macropodine, *M. cf. M. titan*, maintains high levels of bending resistance all along the shaft in both bending axes. This cranio-caudal resistance of the fourth metatarsal of *S. stirlingi* is echoed in both its external and internal cross-sectional anatomy: there is a cranio-medial ridge along the proximal two-thirds of the bone, seen as a large protruding area of cortical bone on the cross-sections. Medial strengthening of the leg bones supports the hypothesis of bipedal striding: in humans, weight is shifted to the medial side of the foot during bearing weight on one leg at a time.

Sthenurines and macropodines also differ in the bending stresses of the phalanges, with sthenurines in general showing greater resistances. The cross-sectional anatomy of the proximal phalanx shows *S. stirlingi* to have a greater extent of medial thickening of bone at the distal end, while in *M. cf. M. titan* it is the lateral side that shows the greater thickening. Again, this supports the hypothesis that sthenurine anatomy was adapted to bearing weight on one leg at a time.

The basal late Miocene sthenurine *Hadronomas* shows a basically sthenurine pattern in its resistance to bending stresses, but with some macropodine features (e.g., in the similarity to macropodines of some of the values for medio-lateral bending resistances), possibly reflecting its retention of the fifth pedal digit. However, aspects of the morphology of both the fourth metatarsal, with evidence of cranio-medial thickening, and the calcaneum, with the lack of plantar thickening of cortical bone, are indicative of a mode of locomotion like that of the monodactyl sthenurines. Additionally, the external morphology of the calcaneum resembles that of the monodactyl sthenurines in ways indicative of a similar type of locomotion (Janis et al., 2021).

The macropodine *Protemnodon* is divergent from the other macropodines studied here in its pattern of bending resistances, and divergent from all of the taxa in both the anatomy, and the pattern of bending resistances, of the intermediate phalanx. The distribution of cortical bone in its calcaneal tuber does not indicate the type of high resistance seen in *Macropus*, and casts further doubt on it being primarily a hopping mammal (see Den Boer, 2018; Jones, 2020).

Clearly large kangaroos (i.e., >25kg) in the past had a much greater diversity of locomotor modes than seen in extant large macropods, as also shown by the recent study of the large, but probably arboreal, Pleistocene macropodine (related to *Protemnodon*) *Congruus kitcheneri* (Warburton & Prideaux, 2021).

## ACKNOWLEDGMENTS

We thank Jin Meng and Judy Galkin (Vertebrate Paleontology) at the American Museum of Natural History (New York, USA) for access to specimens in their care, and Ruth O'Leary and Ana Balcarel for facilitating the scans of *M. giganteus* and *S. stirlingi* (and thanks to all, plus Alana Gishlik, for the loan of the foot of *P. brehus*). We thank other museum curators for loans of specimens in their care for the measurements used in the body mass estimations: Pip Brewer, Roula Pappa, and

Nadine Gabriel at the Natural History Museum (London, UK); Helen Ryan and Kenny Travouillon at the Western Australian Museum (Perth, Australia); Adam Yates at the Museum and Art Gallery of the Northern Territory (Alice Springs, Australia); and Rob Asher and Mathew Lowe at the University of Cambridge Museum of Zoology (Cambridge, UK). Additional thanks to curators who provided access to their collections for the measurements for body mass estimations: Heather Janetizki, Kirsten Spring, Scott Hocknull, and Andrew Rozefelds (Queensland Museum, Brisbane, Australia); Sandy Ingleby and Anja Divaljan (Australian Museum, Sydney, Australia); Erich Fitzgerald, David Pickering, Tom Rich, and Karen Roberts (Museum Victoria, Melbourne, Australia); Claire Stevenson, Ric How, and Alex Bayes (Western Australian Museum, Perth, Australia) and Catherine Kemper, David Stemmer, and Mary-Anne Binnie (South Australian Museum, Adelaide, Australia). For the scanning of the loaned specimens at the University of Bristol we thank Tom Davies and Liz Martin-Silverstone. And finally, thanks to Billie Jones for the phylogeny and reconstructions (Figure 1), to Nuria Melisa Morales-García ([www.sciencegraphicdesign.com](http://www.sciencegraphicdesign.com)) for rendering the graphical abstract, and to Hazel Richards, at Museum Victoria (Melbourne, Australia) for taking the photographs of *M. ferragus* and *S. stirlingi* (in the Data S2). Funds from the University of Bristol Program in Palaeobiology enabled the scans and the return shipping of specimens. Funds to CMJ from the Bushnell Foundation (Brown University) aided in the collection of linear measurement data for the body mass estimations.

## AUTHOR CONTRIBUTIONS

**Amber Y. Wagstaffe:** Data curation (equal); formal analysis (equal); investigation (equal); methodology (equal); project administration (equal); validation (equal); visualization (equal); writing – original draft (lead); writing – review and editing (supporting). **Adrian M. O'Driscoll:** Data curation (equal); formal analysis (equal); investigation (equal); methodology (equal); project administration (equal); validation (equal); visualization (equal); writing – original draft (supporting); writing – review and editing (supporting). **Callum J. Kunz:** Data curation (equal); formal analysis (equal); investigation (equal); methodology (equal); project administration (equal); validation (equal); visualization (equal); writing – original draft (supporting); writing – review and editing (supporting). **Emily J. Rayfield:** Data curation (equal); funding acquisition (equal); methodology (equal); project administration (equal); resources (equal); software (lead); supervision (equal); writing – original draft (supporting); writing – review and editing (supporting). **Christine M. Janis:** Conceptualization (lead); funding acquisition (equal); investigation (equal); project administration (equal); resources (equal); supervision (equal); writing – original draft (supporting); writing – review and editing (lead).

## PEER REVIEW

The peer review history for this article is available at <https://publons.com/publon/10.1002/jmor.21445>.

## DATA AVAILABILITY STATEMENT

All relevant data are available in the supplementary information.

## ORCID

Amber Y. Wagstaffe  <https://orcid.org/0000-0002-8248-3370>

## REFERENCES

- Aiello, L., & Dean, C. (1990). *An introduction to human evolutionary anatomy*. Academic Press.
- Anderson, J. F., Hall-Martin, A., & Russell, D. A. (1985). Long-bone circumference and weight in mammals, birds and dinosaurs. *Journal of Zoology*, 205, 53–61.
- Anyonge, W. (1993). Body mass in large extant and extinct carnivores. *Journal of Zoology*, 231, 339–350. <https://doi.org/10.1111/j.1469-7998.1993.tb01922.x>
- Baudinette, R. V. (1994). Locomotion in macropodoid marsupials: Gaits, energetics, and heat balance. *Australian Journal of Zoology*, 42, 103–123.
- Baudinette, R. V., Snyder, G. K., & Frappelle, P. B. (1992). Energetic cost of locomotion in the tammar wallaby. *American Journal of Physiology*, 262, R771–R778.
- Bennett, M. B. (2000). Unifying principles in terrestrial locomotion: Do hopping Australian marsupials fit in? *Physiological and Biochemical Zoology*, 73, 726–735.
- Bennett, M. B., & Taylor, G. C. (1995). Scaling of elastic strain energy in kangaroos and the benefits of being big. *Nature*, 378, 56–59.
- Bertram, J. E. A., & Biewener, A. A. (1988). Bone curvature: Sacrificing strength for load predictability? *Journal of Theoretical Biology*, 131, 75–92.
- Biewener, A. A. (2005). Review: Biomechanical consequences of scaling. *Journal of Experimental Biology*, 208, 1665–1676. <https://doi.org/10.1242/jeb.01520>
- Biewener, A. A. (2008). Tendons and ligaments: Structure, mechanical behavior and biological function. In *Collagen* (pp. 269–284). Springer.
- Biewener, A. A., & Baudinette, R. V. (1995). In vivo muscle force and elastic energy storage during steady-speed hopping of tammar wallabies (*Macropus eugenii*). *Journal of Experimental Biology*, 198, 1829–1841.
- Blickhan, R., & Full, R. J. (1993). Similarity in multilegged locomotion: Bouncing like a monopode. *Journal of Comparative Physiology A*, 173, 509–517.
- Burk, A., & Springer, M. S. (2000). Intergeneric relationships among Macropodoidea (Metatheria: Diprotodontia) and the chronicle of kangaroo evolution. *Journal of Mammalian Evolution*, 7, 213–237. <https://doi.org/10.1023/A:1009488431055>
- Burk, A., Westerman, M., & Springer, M. (1998). The phylogenetic position of the musky rat-kangaroo and the evolution of bipedal hopping in kangaroos (Macropodidae: Diprotodontia). *Systematic Biology*, 47, 457–474. <https://doi.org/10.1080/106351598260824>
- Butler, K., Travouillon, K. J., Evans, A. R., Murphy, L., Price, G. J., Archer, M., Hand, S. J., & Weisbecker, V. (2021). 3D morphometric analysis reveals similar ecomorphs for early kangaroos (Macropodidae) and fanged kangaroos (Balbaridae) from the Riversleigh World Heritage Area, Australia. *Journal of Mammalian Evolution*, 28, 199–219. <https://doi.org/10.1007/s10914-020-09507-8>
- Butler, K., Travouillon, K. J., Price, G. J., Archer, M., & Hand, S. J. (2017). Species abundance, richness, and body size evolution of kangaroos (Marsupialia: Macropodiformes) through the Oligo-Miocene of Australia. *Palaeogeography, Palaeoclimatology, Palaeoecology*, 487, 25–36. <https://doi.org/10.1016/j.palaeo.2017.08.016>
- Camens, A. B., & Worthy, T. H. (2019). Walk like a kangaroo: New fossil trackways reveal a bipedally striding macropodid in the Pliocene of Central Australia. *Journal of Vertebrate Paleontology, Programs and Abstracts*, 2019, 72.
- Campione, N. E., & Evans, D. C. (2012). A universal scaling relationship between body mass and proximal limb bone dimensions in quadrupedal terrestrial tetrapods. *BMC Biology*, 10, 60. <https://doi.org/10.1186/1741-7007-10-60>
- Cascini, M., Mitchell, K. J., Cooper, A., & Phillips, M. J. (2019). Reconstructing the evolution of giant extinct kangaroos: Comparing the utility of DNA, morphology, and total evidence. *Systematic Biology*, 68, 520–537. <https://doi.org/10.1093/sysbio/syy080>
- Cavagna, G. A., Heglund, N. C., & Taylor, C. R. (1977). Mechanical work in terrestrial locomotion: Two basic mechanisms for minimizing energy expenditure. *American Journal of Physiology*, 233, R243–R261.
- Couzens, A. M., & Prideaux, G. J. (2018). Rapid Pliocene adaptive radiation of modern kangaroos. *Science*, 362, 72–75. <https://doi.org/10.1126/science.aas8788>
- Dawson, R. S., Warburton, N. M., Richards, H. L., & Milne, N. (2015). Walking on five legs: Investigating tail use during slow gait in kangaroos and wallabies. *Australian Journal of Zoology*, 63, 192–200. <https://doi.org/10.1071/ZO15007>
- Dawson, T. J. (1983). *Monotremes and marsupials: The other mammals*. Edward Arnold.
- Dawson, T. J., & Taylor, C. R. (1973). Energetic cost of locomotion in kangaroos. *Nature*, 246, 313–314. <https://doi.org/10.1038/246313a0>
- Den Boer, W. (2018). *Evolutionary progression of the iconic Australasian kangaroos, rat-kangaroos, and their fossil relatives (Marsupialia: Macropodiformes)* [Dissertation, Uppsala University, Uppsala].
- Den Boer, W., & Kear, B. P. (2018). Is the fossil rat-kangaroo *Palaeopotorous priscus* the most basally branching stem macropodiform? *Journal of Vertebrate Paleontology*, 38, e1428196. <https://doi.org/10.1080/02724634.2017.1428196>
- Dick, T. J., & Clemente, C. J. (2017). Where have all the giants gone? How animals deal with the problem of size. *PLoS Biology*, 15, e2000473. <https://doi.org/10.1371/journal.pbio.2000473>
- Doube, M., Felder, A. A., Chua, M. Y., Lodhia, K., Koslowski, M. M., Hutchinson, J. R., & Shefelbine, S. J. (2018). Limb bone scaling in hopping macropods and quadrupedal artiodactyls. *Royal Society Open Science*, 5, 180152. <https://doi.org/10.1098/rsos.180152>
- Doube, M., Kłosowski, M. M., Arganda-Carreras, I., Cordelières, F., Dougherty, R. P., Jackson, J., Schmid, B., Hutchinson, J. R., & Shefelbine, S. J. (2010). BoneJ: Free and extensible bone image analysis in ImageJ. *Bone*, 47, 1076–1079. <https://doi.org/10.1016/j.bone.2010.08.023>
- Flannery, T. F. (1980). *Macropus mundjabus*, a new kangaroo (Marsupialia: Macropodidae) of uncertain age from Victoria, Australia. *Australian Mammalogy*, 3, 35–51.
- Harcourt-Smith, W. E., & Aiello, L. C. (2004). Fossils, feet and the evolution of human bipedal locomotion. *Journal of Anatomy*, 204, 403–416. <https://doi.org/10.1111/j.0021-8782.2004.00296.x>
- Helgen, K. M., Wells, R. T., Kear, B. P., Gerdtz, W. R., & Flannery, T. F. (2006). Ecological and evolutionary significance of sizes of giant extinct kangaroos. *Australian Journal of Zoology*, 54, 293–303. <https://doi.org/10.1071/ZO0507>
- Hocknull, S. A., Lewis, R., Arnold, L. J., Pietsch, T., Joannes-Boyau, R., Price, G. J., Moss, P., Wood, R., Dosseto, A., Louys, J., Olley, J., & Lawrence, R. A. (2020). Extinction of eastern Sahul megafauna coincides with sustained environmental deterioration. *Nature Communications*, 11, 1–14. <https://doi.org/10.1038/s41467-020-15785-w>
- Howell, A. B. (1965). *Speed in animals*. Hafner.
- Jackson, S., & Vernes, K. (2010). *Kangaroo: A portrait of an extraordinary marsupial*. Allen and Unwin.
- Janis, C. M., & Bernor, R. L. (2019). The evolution of equid monodactyly: A review including a new hypothesis. *Frontiers in Ecology and Evolution*, 7, 119. <https://doi.org/10.3389/fevo.2019.00119>
- Janis, C. M., Buttrill, K., & Figueirido, B. (2014). Locomotion in extinct giant kangaroos: Were sthenurines hop-less monsters? *PLoS One*, 9, e109888. <https://doi.org/10.1371/journal.pone.0109888>
- Janis, C. M., Napoli, J. G., Billingham, C., & Martín-Serra, A. (2020). Proximal humerus morphology indicates divergent patterns of locomotion in extinct giant kangaroos. *Journal of Mammalian Evolution*, 27, 627–647. <https://doi.org/10.1007/s10914-019-09494-5>

- Janis, C. M., O'Driscoll, A., & Richards, H. (2021). Did Miocene didactyl sthenurine kangaroos walk like the Plio-Pleistocene didactyl ones? *Journal of Vertebrate Paleontology, Programs and Abstracts*, 2021, 148.
- Jashashvili, T., Dowdeswell, M. R., Lebrun, R., & Carlson, K. J. (2015). Cortical structure of hallucal metatarsals and locomotor adaptations in hominoids. *PLoS One*, 10, e0117905. <https://doi.org/10.1371/journal.pone.0117905>
- Jones, B. (2020). Locomotor divergence in Macropodoidea: Proteomnodon was not a giant hopping kangaroo [Masters' thesis, University of Bristol, Bristol, UK].
- Jones, B., Martín-Serra, A., Rayfield, E. J., & Janis, C. M. (2021). Distal humeral morphology indicates locomotory divergence in extinct giant kangaroos. *Journal of Mammalian Evolution*. <https://doi.org/10.1007/s10914-021-09576-3>
- Kear, B. P., & Cooke, B. N. (2001). A review of macropodoid systematics with the inclusion of a new family. *Memoirs of the Association of Australasian Palaeontologists*, 25, 83–101.
- Kear, B. P., Lee, M. S. Y., Gerditz, W. R., & Flannery, T. F. (2008). Evolution of hind limb proportions in kangaroos (Marsupialia: Macropodoidea). In E. J. Sargis & M. Dagosto (Eds.), *Mammalian evolutionary morphology: A tribute to Fredrick S. Szalay* (pp. 25–35). Springer Science.
- Kimura, T. (2003). Differentiation between fore- and hindlimb bones and locomotor behaviour in primates. *Folia Primatologica*, 74, 17–32. <https://doi.org/10.1159/000068391>
- Llamas, B., Brotherton, P., Mitchell, K. J., Templeton, J. E. L., Thomson, V. A., Metcalf, J. L., Armstrong, K. N., Kasper, M., Richards, S. M., Camens, A. B., Lee, M. S. Y., & Cooper, A. (2015). Late Pleistocene Australian marsupial DNA clarifies the affinities of extinct megafaunal kangaroos and wallabies. *Molecular Biology and Evolution*, 32, 574–584. <https://doi.org/10.1093/molbev/msu338>
- Marchi, D. (2005). The cross-sectional geometry of the hand and foot bones of the Hominoidea and its relationship to locomotor behavior. *Journal of Human Evolution*, 49, 743–761. <https://doi.org/10.1016/j.jhevol.2005.08.002>
- McGowan, C. P., Baudinette, R. V., & Biewener, A. A. (2008). Differential design for hopping in two species of wallabies. *Comparative Biochemistry and Physiology, A*, 150, 151–158. <https://doi.org/10.1016/j.cbpa.2006.06.018>
- McGowan, C. P., Skinner, J., & Biewener, A. A. (2008). Hind limb scaling of kangaroos and wallabies (superfamily Macropodoidea): Implications for hopping performance, safety factor, and elastic scaling. *Journal of Anatomy*, 212, 153–163. <https://doi.org/10.1111/j.1469-7580.2007.00841.x>
- McHorse, B. K., Biewener, A. A., & Pierce, S. E. (2017). Mechanics of evolutionary digit reduction in fossil horses (Equidae). *Proceedings of the Royal Society B*, 284, 20171174. <https://doi.org/10.1098/rspb.2017.1174>
- Mitchell, D. R., & Wroe, S. (2019). Biting mechanics determines craniofacial morphology among extant diprotodont herbivores: Dietary predictions for the giant extinct short-faced kangaroo, *Simosthenurus occidentalis*. *Paleobiology*, 45, 167–181. <https://doi.org/10.1017/pab.2018.46>
- Mitchell, K. J., Pratt, R. C., Watson, L. N., Gibb, G. C., Llamas, B., Kasper, M., Edson, J., Hopwood, B., Male, D., Armstrong, K. N., & Meyer, M. (2014). Molecular phylogeny, biogeography, and habitat preference evolution of marsupials. *Molecular Biology and Evolution*, 31, 2322–2330. <https://doi.org/10.1093/molbev/msu176>
- Murray, P. (1991). The sthenurine affinity of the late Miocene kangaroo, *Hadronomas puckeridgei* Woodburne (Marsupialia, Macropodidae). *Alcheringa*, 15, 255–283.
- Murray, P. F. (1995). The postcranial skeleton of the Miocene kangaroo, *Hadronomas puckeridgei* Woodburne (Marsupialia, Macropodidae). *Alcheringa*, 19, 119–170.
- O'Connor, S., Dawson, T., Kram, R., & Donelan, J. (2014). The kangaroo's tail propels and powers pentapedal locomotion. *Biology Letters*, 10, 20140381. <https://doi.org/10.1098/rsbl.2014.0381>
- Pollock, C. M., & Shadwick, R. E. (1994). Allometry of muscle, tendon, and elastic energy storage capacity in mammals. *The American Journal of Physiology-Regulatory, Integrative and Comparative Physiology*, 266, R1022–R1031. <https://doi.org/10.1152/ajpregu.1994.266.3.R1022>
- Prideaux, G. J. (2004). Systematics and evolution of the sthenurine kangaroos. *University of California. Publications in Geological Science*, 146, 1–623.
- Prideaux, G. J., & Warburton, N. M. (2010a). An osteology-based appraisal of the phylogeny and evolution of kangaroos and wallabies (Macropodidae: Marsupialia). *Zoological Journal of the Linnean Society*, 159, 954–987. <https://doi.org/10.1111/j.1096-3642.2009.00607.x>
- Prideaux, G. J., & Warburton, N. M. (2010b). Functional pedal morphology of the extinct tree-kangaroo *Bohra* (Diprotodontia: Macropodidae). In M. D. B. Eldridge & G. M. Coulson (Eds.), *Macropods: The biology of kangaroos, wallabies and rat-kangaroos* (pp. 137–151). CSIRO.
- Reynolds, P. S. (2002). How big is a giant? The importance of method in estimating body size of extinct mammals. *Journal of Mammalogy*, 83, 321–332. [https://doi.org/10.1644/1545-1542\(2002\)083<0321:HBIAGT>2.0.CO;2](https://doi.org/10.1644/1545-1542(2002)083<0321:HBIAGT>2.0.CO;2)
- Snelling, E. P., Biewener, A. A., Hu, Q., Taggart, D. A., Fuller, A., Mitchell, D., Maloney, S. K., & Seymour, R. S. (2017). Scaling of the ankle extensor muscle-tendon units and the biomechanical implications for bipedal hopping locomotion in the post-pouch kangaroo *Macropus fuliginosus*. *Journal of Anatomy*, 231, 921–930. <https://doi.org/10.1111/joa.12715>
- Tedford, R. H. (1967). The fossil Macropodidae from Lake Menindee, New South Wales. *University of California. Publications in Geological Science*, 64, 1–156.
- Wagstaffe, A. Y. (2018). The biomechanics of kangaroo feet: Hopping for a better resolution [Masters' thesis, University of Bristol, Bristol, UK].
- Warburton, N. M., & Prideaux, G. J. (2021). The skeleton of *Congruus kitcheneri*, a semiarborescent kangaroo from the Pleistocene of southern Australia. *Royal Society Open Science*, 8, 202216. <https://doi.org/10.1098/rsos.202216>
- Warbuton, N. M., Yakovlev, M., & Malric, A. (2012). Anatomical adaptations of the hind limb musculature of tree-kangaroos for arboreal locomotion (Marsupialia: Macropodinae). *Australian Journal of Zoology*, 60, 246–258. <https://doi.org/10.1071/ZO12059>
- Wells, R. T., & Tedford, R. H. (1995). *Sthenurus* (Macropodidae, Marsupialia) from the Pleistocene of Lake Callabonna, South Australia. *Bulletin of the American Museum of Natural History*, 225, 1–111.
- Westerman, M., Burk, A., Amrine-Madsen, H. M., Prideaux, G. J., Case, J. A., & Springer, M. S. (2002). Molecular evidence for the last survivor of an ancient kangaroo lineage. *Journal of Mammalian Evolution*, 9, 209–223.
- Windsor, D. E., & Dagg, A. I. (1971). The gaits of the Macropodinae (Marsupialia). *Journal of Zoology*, 163, 165–175. <https://doi.org/10.1111/j.1469-7998.1971.tb04530.x>

## SUPPORTING INFORMATION

Additional supporting information may be found in the online version of the article at the publisher's website.

**How to cite this article:** Wagstaffe, A. Y., O'Driscoll, A. M., Kunz, C. J., Rayfield, E. J., & Janis, C. M. (2022). Divergent locomotor evolution in “giant” kangaroos: Evidence from foot bone bending resistances and microanatomy. *Journal of Morphology*, 283(3), 313–332. <https://doi.org/10.1002/jmor.21445>